2020

Examining morphological differences in Heschl's gyrus between neurotypical and dyslexic brains

BOSTON UNIVERSITY

SARGENT COLLEGE OF HEALTH AND REHABILITATION SCIENCES

Thesis

EXAMINING MORPHOLOGICAL DIFFERENCES IN HESCHL'S GYRUS BETWEEN NEUROTYPICAL AND DYSLEXIC BRAINS

by

JAMIE A. CHIN

B.S., Loyola University Chicago, 2013

Submitted in partial fulfillment of the

requirements for the degree of

Master of Science

2020

Approved by

First Reader _____

Tyler K. Perrachione, Ph.D.
Associate Professor of Speech, Language, and Hearing Sciences

Second Reader _____

Alyssa Boucher, Ph.D., CCC-SLP
Clinical Assistant Professor of Speech, Language, and Hearing Sciences

Third Reader _____

Gabrielle-Ann Torre, Ph.D.
Post-doctoral Fellow
Communication Neuroscience Research Laboratory

ACKNOWLEDGMENTS

I would first like to thank my committee, Dr. Tyler Perrachione, Dr. Alyssa Boucher, and Dr. Gabrielle-Ann Torre. You have all given me an immense amount of support and encouragement. Due to your guidance, I have grown as a researcher and have really realized how capable I am. You inspire me to continue to think critically and creatively.

Thank you to the members of the Communication Neuroscience Research Laboratory. I always felt welcome to reach out and ask questions. Being witness to all of your individual scientific endeavors invigorated me in my own. Thank you especially to Alex Kapadia. You always made yourself available and were an invaluable peer support and mentor, being someone who had completed the thesis process herself. And thank you to Maya Saupe who continually encouraged me and urged me on when I felt overwhelmed.

I would also like to thank the faculty and students of the Speech-Language Pathology Department at Sargent College. You were all so caring, supportive, and interested in my progress. I look forward to working alongside you all as colleagues.

Finally, I must thank my family, friends, and my partners, Lilian Haymann and Jeffrey Crenshaw. You provided unwavering support and nurturing, literally and figuratively. I likely would not have made it without you two. Thank you for always having faith in me even when I did not.

EXAMINING MORPHOLOGICAL DIFFERENCES IN HESCHL'S GYRUS BETWEEN NEUROTYPICAL AND DYSLEXIC BRAINS

JAMIE A. CHIN

ABSTRACT

Current methods of diagnosis for developmental dyslexia rely on family history report and cognitive and language behavioral testing. However, relying on these measures alone to predict dyslexia in at-risk children can result in low sensitivity and specificity, with dyslexic individuals either being missed or over-identified. Prediction accuracy could be increased by considering structural differences in the dyslexic brain along with behavioral measures. Reduplication of Heschl's gyrus, where the primary auditory cortex resides, has been suggested as a risk factor for developing dyslexia. The current investigation explored if differences in interhemispheric duplication patterns and gray matter volume of Heschl's gyrus could distinguish between dyslexic and neurotypical (control) brains. A detailed labeling protocol based on macroanatomical landmarks and explicitly defined reduplication morphotypes: single Heschl's gyrus (SH), common stem duplication (CSD), complete posterior duplication (CPD), and multiple duplication (MD) was developed. Overall, there was no significant difference in the incidence of morphotypes between control and dyslexic brains. Duplication of Heschl's gyrus was a common occurrence in both groups. However, results suggest that the MD morphotype may occur more often in dyslexic brains. Gray matter volume of anterior Heschl's gyrus was larger in the left hemisphere in both groups but tended to be larger overall in dyslexic brain. Results of this investigation confirmed the presence of high morphological variability between and within

brains and suggest that reduplications in Heschl's gyrus alone are not enough to designate between neurotypical and dyslexic brains. It is likely that developmental dyslexia has heterogeneous origins, and it is possible that increased gyrification combined with other structural differences is one possible origin.

TABLE OF CONTENTS

ACKNOWLEDGMENTS iv

ABSTRACT v

TABLE OF CONTENTS vii

LIST OF TABLES ix

LIST OF FIGURES x

LIST OF ABBREVIATIONS xii

INTRODUCTION 1

1.1 Developmental Dyslexia 1

1.2 Significance of Heschl's Gyrus 4

1.2.1 Location of Primary Auditory Cortex & Connection to Planum Temporale 4

1.2.2 Review of HG in Controls: Morphology and Duplication Patterns in the General Population 12

1.2.3 Review of HG in Specialized and Disordered Populations 14

1.2.3.1 Musicians 15

1.2.3.2 Phoneticians 16

1.2.3.3 Schizophrenia 17

1.3 Purpose of Current Study 18

METHODS 20

2.1 Participants 20

2.2 Image Analysis 21

2.2.1 Classification of Heschl's Gyrus 21

2.2.2 Labels & Volume Measurements 24
2.2.3 Data Analysis 27
2.2.3.1 Distribution of HG Morphotypes 27
2.2.3.2 HG Gray Matter Volume 27
RESULTS 29
3.1 Distribution of Morphotypes 29
3.2 HG Gray Matter Volume 33
3.2.1 Total HG Volume 33
3.2.2 First and Second Heschl's Gyri Volumes 36
3.2.3 Hemispheric HG Asymmetry 39
DISCUSSION 41
4.1 Summary of Results and Clinical Applications 41
4.2 Considerations from the Labeling Protocol Adopted for this Study 44
4.3 Limitations and Future Directions 48
CONCLUSION 51
REFERENCES 53
VITA 57

LIST OF TABLES

Table 1.1 Review of previous and current protocols for labeling HG…….…….. 6

Table 2.1 Subject demographics and behavioral scores…… 21

Table 3.1 Distribution of HG morphotypes by hemisphere for each group…… 30

Table 3.2 Number and percentage of interhemispheric HG patterns by morphotype... 32

Table 3.3 Number and percentage of interhemispheric HG patterns as “single” or “duplicated”…… 32

Table 3.4 HG lateralization across groups……..…… 40

Table 3.5 Mean Asymmetry Index (AI)…….…… 40

LIST OF FIGURES

Figure 2.1 View of Heschl's gyrus…… 22

Figure 2.2 Identifying landmarks seen on the pial surface of the superior temporal plane……. 23

Figure 2.3 Appearance of HG in sagittal planes…… 24

Figure 2.4 Outlines of surface labels…… 26

Figure 3.1 Distributions of HG morphotypes in control and dyslexic brains…… 30

Figure 3.2 Distribution of single and reduplicated gyri in control and dyslexic brains.. 31

Figure 3.3 Distribution of HG duplication patterns across hemispheres for all subjects. 32

Figure 3.4 Total HG volume across group and hemisphere…… 34

Figure 3.5 Total HG volume across group and hemisphere excluding MD…… 34

Figure 3.6 Total HG volume in each morphotype across hemispheres for all subjects… 35

Figure 3.7 Total HG volume in "single" and "duplicated" across hemisphere and group……. 35

Figure 3.8 HG1 volume across group and hemisphere…… 37

Figure 3.9 HG1 volume in "single" and "duplicated" across group and hemisphere… 37

Figure 3.10 HG1 volume in "single" and "duplicated" across group and hemisphere excluding MD…… 38

Figure 3.11 HG2 volume across group and hemisphere……. 38

Figure 3.12 Hemispheric lateralization in HG…… 40

Figure 4.1 Sulcus intermedius "o" configuration…… 45

Figure 4.2 First Heschl's sulcus "x" configuration…… 45

Figure 4.3 Morphological variability of HG2 in surface representations…… 46

Figure 4.4 Morphological variability of PT……. 46

Figure 4.5 Morphological variability of MD in surface representations……. 47

LIST OF ABBREVIATIONS

Abbreviation	Full description
aHG	anterior Heschl's gyrus
AI	Asymmetry index
BOLD	blood-oxygen-level dependent
CPD	complete posterior duplication
CSD	common stem duplication
fMRI	functional magnetic resonance imaging
FTS	first temporal sulcus
GM	gray matter
HG	Heschl's gyrus
HG1	first Heschl's gyrus
HG2	second Heschl's gyrus
HS	Heschl's sulcus
HS1	first Heschl's sulcus
HS2	second Heschl's sulcus
LH	left hemisphere
MD	multiple duplication
MR	magnetic resonance
MRI	magnetic resonance imaging
PAC	primary auditory cortex
PT	planum temporale
RAN	rapid automatized naming

RH	right hemisphere
SH	single Heschl's gyrus
SI	sulcus intermedius
STG	superior temporal gyrus
TOWRE	*Test of Word Reading Efficiency*
V	volume
WM	white matter
WRMT-R/NU	*Woodcock Reading Mastery Test -- Revised/Normative Update*

INTRODUCTION

1.1 Developmental Dyslexia

Developmental dyslexia is a communication disorder defined by a difficulty in learning how to accurately and fluently decode written material which develops despite typical or above average intelligence, the absence of other speech-language impairments, and adequate access to classroom instruction (Shaywitz, 1998; Shaywitz & Shaywitz, 2003). This disorder affects 5–15% of the population and extends throughout a person's lifetime, often interfering with academic success (Eckhert et al., 2016). Because of their reading difficulties, children with dyslexia tend to practice reading less outside of the classroom. This can exacerbate the discrepancy in reading skills between children with dyslexia and their peers. Additionally, children with dyslexia will be more severely hindered when their classroom education transitions from "learning to read" to "reading to learn." By adulthood, many who were diagnosed with dyslexia as children have attained the ability to read accurately but still experience effortful reading and difficulties spelling (Waldie et al., 2017). Understanding the signs of developmental dyslexia can lead to earlier implementation of remediation services and classroom support and influence better reading outcomes long term.

While dyslexia is known to have a strong hereditary link, the exact etiology of dyslexia is currently unknown. However, there are some known behavioral risk factors and proposed brain structural differences which can be used to predict the likelihood of developing a reading disorder. Indeed, behavioral measures are typically used to identify at-risk children and confirm diagnosis of dyslexia (Kraft et al. 2016). Developmental dyslexia is characterized by a general weakness in phonological processing and/or in rapid

automatized naming (RAN) (e.g., naming colors, letters, or digits) (Lervåg at al., 2009). Phonological processing, specifically phonemic awareness, refers to how speech sounds are mentally represented, manipulated, stored, and retrieved. Deficits in RAN can be indicative of slower processing speed or an impairment in the retrieval of phonological information. An individual with developmental dyslexia experiencing deficits in one or both of these components will experience difficulty achieving accurate or fluent reading. However, behavioral testing alone can miss (false-negative) or over identify (false-positive) at-risk children. If too many children are falsely identified as having a reading disorder, the level of service and quality of attention given to children who actually have dyslexia is reduced. Thus, criteria for a more accurate diagnosis of dyslexia requires high levels of sensitivity and specificity.

While phonological processing and RAN have shown to be reliable predictors of literacy, a better understanding of structural changes in the dyslexic brain and how they relate to functional behavior could increase diagnostic power and inform more targeted treatment. In order to develop a profile of behavioral and neural differences in pre-literate children considered at-risk for dyslexia, Kraft et al. (2016) implemented behavioral testing to measure abilities that are precursors to reading (e.g., phonological awareness, RAN, visual and verbal working memory) and MR brain imaging to examine structure and connectivity. Then, to assess the prediction accuracy in diagnosing dyslexia with neuroanatomical measures in conjunction with behavioral testing compared to behavioral measures alone, Kraft et al. (2016) re-assessed some of the children after the age of reading acquisition. They found that the accuracy in predicting the development of a reading

disorder increased from 63% to 80% when both brain structure and behavioral measures were used to identify at-risk children. However, the exact brain regions affected in individuals with developmental dyslexia is still a contested subject. Many studies have investigated macrostructural and morphometric differences between dyslexic brains and controls with mixed results (Ramus et al., 2018). Furthermore, it is unknown if morphometric variability gives rise to a reading disorder or develops as a consequence of developmental dyslexia.

Macrostructural differences may be useful in detecting the presence of a reading disorder or other behavioral differences. The development of gyri and sulci occur early in fetal development and are relatively fixed after birth (Dubois et al., 2008). Additionally, gyri and sulci are easily and reliably recognized. Prominent sulci have been used as reliable landmarks when investigating changes in brain structure, particularly in schizophrenia (Ramus et al., 2018). Heschl's gyrus (HG) has been used as a prominent landmark on the superior temporal lobe in studies measuring the human primary auditory cortex (Rademacher et al., 1993). The morphology of HG is highly variable between individuals and hemispheres, and duplications of HG have been associated with phonological disorders, dyslexia (Leonard et al., 1998, 1993), phonological expertise (Golestani et al. 2011), and musical aptitude (Benner et al., 2017). Studies have suggested that reduplications of HG occur more frequently in dyslexia. Leonard et al. (2001) identified large HG duplications in the left hemisphere as one of four macrostructural risk factors in predicting dyslexia. Furthermore, Leonard et al. (2006) found that dyslexia was positively associated with overall larger cerebral and auditory cortices. Additional investigation into

the differences in HG morphology between control and dyslexic brains may reveal a reliable diagnostic landmark.

1.2 Significance of Heschl's Gyrus

1.2.1 Location of Primary Auditory Cortex & Connection to Planum Temporale

The morphology of the superior temporal gyrus (STG) varies greatly between individuals and between hemispheres. HG is a well-studied landmark on the STG. It can be seen as a prominent omega-shaped (Ω) bulge in sagittal views of the brain traveling along the Sylvian fissure, terminating at the insula. Similarly, HG can be recognized in coronal views as a bulge between the parietal and temporal lobes, moving laterally along the lower portion of the Sylvian fissure. In the transverse or axial plane, HG extends antero-laterally and postero-medially (Yousry et al., 1997). In humans, the primary auditory cortex (PAC) is proposed to be principally located within HG (Rademacher et al., 1993). Several studies have confirmed that the PAC is situated in HG through functional BOLD (blood-oxygen-level-dependent activity) *in vivo* and cellular structure in post-mortem cytoarchitecture (Da Costa et al., 2011). Some have also proposed functionally distinct roles for right and left HG, with temporal information, such as such as speech, processed predominately in left HG, whereas spectral information, like musical pitch, is processed predominately in right HG (Golestani & Pallier, 2007; Golestani et al., 2007, 2011; Schneider et al., 2005). Posterior to HG is a region of the brain called planum temporale (PT), thusly named due to its plane-like, flat appearance. The PT is a major region involved in language processing, including phonological processing and language comprehension (Altarelli et al., 2014; Shapleske et al., 1998). In typical human brains, there tends to be a

leftward asymmetry in PT, which correlates with the theory of left lateralized language centers in the brain.

The morphology of HG is highly variable and is most commonly observed in one of three configurations: a single gyrus (SH), common stem duplication (CSD), and complete posterior duplication (CPD) (Abdul-Kareem & Sluming, 2008; Leonard et al., 1998). A CSD configuration is marked by two gyri split by a sulcus intermedius (SI) which typically extends through the lateral first- to second-third of HG but terminates before the most medial end of HG. Both SH and CSD configurations are divided from PT by Heschl's sulcus (HS). The CPD configuration is defined by two distinct gyri separated completely by first Heschl's sulcus (HG1). CPD of HG are separated from PT by a second Heschl's sulcus (HS2). However, there have also been reports of multiple duplications (≥ 3) with as many as five gyri identified (Benner et al., 2017). In their investigation of HG, Benner et al. (2017) observed several instances of multiple duplications in their subjects, designating this morphotype "MD." MD are typically combinations of SH, CSD, and CPD, containing several intermediate sulci and sometimes appearing as an S- or Z- shape when viewed on the superior temporal plane. The identification and quantification of HG morphotypes has been complicated by varying study designs and rater subjectivity. In some studies, additional Heschl's gyri are considered to be part of PT; the stem of CSD is inconsistently considered part of the anterior HG (aHG) or the posterior HG depending on the study (Tzourio-Mazoyer & Mazoyer, 2017). Traditionally, when measuring PAC size in brains with HG duplications, PAC is believed to reside in the most anterior HG; secondary HG are included in PT (Leonard et al., 1998; Wong et al., 2008). However, Da Costa et al.

(2011) observed that functional tonotopic maps of the PAC correlate with HG morphology and that the PAC spans additional gyri in cases of HG duplication. This suggests that the borders of the PAC are not necessarily confined to anatomical boundaries (Da Costa et al., 2011). Further, Da Costa et al. (2011) suggested that duplications of HG represent a functional continuum instead of distinct, independent regions. A summary of various labeling criteria from hallmark studies of HG and PT morphology is reviewed in **Table 1.1**.

Table 1.1. Review of previous and current protocols for labeling HG. The boundaries and labels of HG have been variable across investigations. This makes it difficult to reach a consensus on the frequency of HG morphotypes and total volume across populations.

Authors (Year)	Study Population	Region	Label Name	Criteria for HG Boundaries
Rademacher et al. (1993)	Preserved brain tissue, controls	Brodmann Area 41	**H1:** Heschl's gyrus	Rostral border corresponds to first transverse sulcus; posterior border corresponds to HS, HG is bordered medially by medial margin of temporal lobe adjacent to insula; lateral border corresponds to external lip of sylvian fissure and does not extend to lateral surface of temporal lobe. Planum polare is located rostrally, PT posteriorly, and STG laterally; if there was an "intermediate transverse sulcus" that extended ⅓ to ½ along the axis of the gyrus, considered as a single gyrus with an indented crown
			H2: second transverse gyrus	Gyrus posterior to H1
			H3: third transverse gyrus	Gyrus posterior to H2
Penhune et al. (1996)	Controls	PAC	**PAC-r**	Posterior boundary corresponds to HS or SI when it extends at least ½ length of HG; posterior-medial boundary corresponds to a line drawn from the

				medial end of the first transverse sulcus to the medial end of HS; anterior-lateral boundary is determined by extending lines of first transverse sulcus and HS to lateral end of temporal plane; inferior boundary is determined by drawing a line from the depth of HS to a notch created by the meeting of the superior surface of HG and its stem in sagittal and coronal views
Schneider et al. (2005)	Musicians (professional & amateur), Non-musicians	HG, PT, aSTG	**Anterior gyrus**	Anterior border corresponds to first transverse sulcus and posterior border corresponds to first cHS; divided into three subdivisions: mHG, lHG, and aSTG
			cHS: complete Heschl's sulcus	Demonstrates clear lateral indentation, divides auditory cortex antero-laterally into two parts: (1) HG and aSTG and (2) PT
			mHG: medial portion of HG	Medial ⅔ of HG along mediolateral direction, estimated extend of PAC
			lHG: lateral portion of HG	Remaining part of gyrus between aSTG and mHG
			aSTG: anterior STG	Separated from HG by line y = 0 in stereotaxic coordinates for map of auditory cortex averaged from 87 brains
			PD	Complete posterior duplication is considered part of PT
Golestani et al. (2007)	Monolingual controls	Parietal lobes, HG-PAC	**HG**	HG borders defined by criteria described be Penhune et al. (1996); if multiple transverse gyri were present, only most anterior gyrus was measured; in presence of SI less than ½ length of HG, only most anterior gyral subregion was measured

Wong et al. (2008)	Controls (non-tonal)	HG	**Anterior HG**	Anterior border corresponds to first transverse sulcus; posterior border corresponds to first HS; presence of a SI greater than ½ of aHG without extending completely lateral-medially constituted a "complete duplication," and only most anterior HG was measured SI extending less than ½ HG constituted a "split HG" and entire HG was included in measurements
Warrier et al. (2009)	Controls	HG	**HG**	Anterior limit corresponds to first transverse sulcus, posterior limit corresponds with HS; if SI was present and extended ½ the length of the gyrus, was considered an HG duplication; SI that was less than ½ was not considered a duplication. In presence of SI, line was drawn extending SI to gyral base and the gyrus anterior to this line was considered HG.
Marie et al. (2015)	Controls	HG	**aHG:** anterior HG	Follow transverse temporal sulcus to its antero-lateral limit and draw a horizontal line from the point where HG disappears on sagittal slices through to the lateral edge of the brain.
			postHG: posterior HG	Second gyrus in CPD configurations
			totHG: total HG	Sum of aHG and postHG
			Single HG	HS is the posterior border of aHG, medially, HS joins with temporal transverse sulcus
			CSD: common stem duplication	Presence of SI of Beck which runs parallel to HS and divides lateral part of HG without reaching medial end; SI was at least ⅓ length of HG; two lateral gyri merge at medial ends; heart shape can be seen on sagittal slides; posterior limit of aHG created by following SI and drawing antero-posterior line joining SI and HS

			CPD: complete posterior duplication	Presence of second HS which runs along HG and reaches medial end; "m" shape can be seen on sagittal and coronal slices; posterior limit is HS
Tzourio-Mazoyer & Mazoyer (2017)	Controls	HG and PT	**aHG:** anterior HG	HG defined by same criteria used by Marie et al. (2015)
			PT	Anterior limit of PT defined by HS; in cases of complete HG duplication, second HS was anterior limit of PT
			PT_{post}: Posterior part of PT	Excludes any duplication of HG
			PT_{tot}: Total PT	Sum of PT_{post} and second HG
			HGPT	Sum of aHG and PT_{tot}
Benner et al. (2017)	Musicians (professional & amateur)	STG, including HG and PT	**aHG:** first anterior HG	Most anterior transverse gyrus of STG, between first transverse sulcus and first Heschl's sulcus, anterior commissure line separates aHG from anterior STG
			Single HG	Single gyrus, presence of SI that is smaller than ⅓ length of aHG
			CSD: common stem duplication	Presence of SI that was at least ⅓ length of aHG, SI did not reach medial end of HG
			CPD: complete posterior duplication	Presence of intermediate HS that does not reach lateral end of HG
			MD: multiple duplications	Presence of two intermediate HS or combinations of CSD/CPD structures containing intermediate HS and SI
			HG total	All transverse gyri posterior to aHG and anterior to first complete HS
			Anterior border of PT	First complete HS

According to animal models of brain function, it is possible that variations in the size and morphology of structures in the human brain may convey functional advantages or disadvantages to an individual (Leonard et al., 1998). Particular attention has been given to the structures of HG and PT and their patterns of asymmetry across both hemispheres. As previously stated, brain regions involved in language processing are historically larger in the left hemisphere, consistent with other evidence that language is a left-lateralized operation. Structural and volumetric changes to both HG and PT may be indicative of deficits in language comprehension and use (Tzourio-Mazoyer & Mazoyer, 2017). HG reduplication may affect the size and function of PT; it has been questioned whether the formation of additional Heschl's gyri comes at the expense of PT and leads to an increase in PAC volume. However, answers to this question are again complicated by differences in labeling criteria and regional boundaries. Tzourio-Mazoyer and Mazoyer (2017) found that HG reduplication did not affect the size of PT when posterior Heschl's gyri were included in the total surface area of PT. PT surface area was affected, however, when posterior gyri were considered independent of PT. When the structures of HG and PT were combined, there was no significant difference in total surface area between cases of SH and duplications. These results suggest that while PT size is affected by how HG is labeled and subdivided, multiplications of Heschl's gyri do not lead to a significant increase in the overall volume of the auditory cortex.

If additional gyri do develop to the detriment of PT, it is possible that individuals identified with language impairments will show a higher frequency of HG duplications. Duplications of HG and SH size in the left hemisphere have been suggested as risk factors

for impairments in phonological processing (Abdul-Kareem & Sluming, 2008). Children with poor phonological awareness and neurodevelopmental disorders have been found to have less planar asymmetry, suggesting that HG duplications may affect the size and extent of lateralization of left PT (Leonard et al., 1998; Tzourio-Mazoyer & Mazoyer, 2017). Leonard et al. (1993) have suggested that HG duplications occur more frequently in families with a history of learning disabilities. In a review of HG structure and the PAC, Abdul-Kareem and Sluming (2008) suggest that HG duplications may be used as a phenotypic marker for studying dyslexia in families. It would be interesting and important to investigate if brain macrostructures can be determined to reliably identify language and learning disorders. As previously discussed, variations in brain structure, combined with behavioral measures, may be able to more accurately predict the development of a language disorder, like dyslexia, and thus allow for the development of earlier and more targeted interventions (Kraft et al., 2016). If at-risk children can be reliably identified, early intervention will help them develop compensatory strategies earlier on and allow them to take advantage of the increased neural plasticity of the younger brain.

While it is known that there is a high degree of variability in the temporal lobes between individuals and hemispheres, the impact of these morphological variations in HG cannot be fully understood without a deeper study of HG's functions. Zatorre (2003) proposed that the combined interaction of a neural system's functional and structural properties may be the best predictor of behavior. By understanding how the shape and function of the auditory and language networks interact, we might better understand how variations HG and PT result in impairments in learning speech, language, and music. First,

the morphology of HG in typically developing individuals must be examined and understood. Then, frequently occurring variations in HG in the typical population can be compared to HG morphology in disordered populations. Overall structural differences may point to a locus of behavioral aberrations.

1.2.2 Review of HG in Controls: Morphology and Duplication Patterns in the General Population

HG morphology has been studied extensively in control populations, offering a better understanding of the patterns of HG duplication in the general population and the implications of HG size and shape on functional skills in typically developing brains.

The most prevalent reported pattern of HG morphology in the general population is the bilateral SH morphotype, with left-lateralized asymmetry and larger left PT (Abdul-Kareem & Slumming, 2008; Marie et al., 2015). However, in a study of 430 subjects, Marie et al. (2015) found that duplications of HG frequently occur, with 64% of hemispheres showing patterns of reduplication, 49% on the right and 37% on the left. According to their findings, in HG reduplications of the left hemisphere, CSD morphotypes are twice as likely to occur as CPD morphotypes. Conversely, in the right hemisphere, HG reduplications are 10% more likely to occur as a CPD morphotype versus a CSD. The authors concluded that the patterns of duplication were, from most frequently occurring to least: bilateral single gyrus (L1/R1), left single with duplicated right (L1/R2), duplicated left with single right (L2/R1), and bilateral reduplications (L2/R2) (Marie et al., 2015). In duplicated configurations, aHG surface area was decreased with an overall increase in total HG surface area. In comparisons between right- and left-handed subjects, HG duplications were observed less in left-handers. However, in instances of reduplication, left-handers

tended to demonstrate greater surface area of the right aHG with increased total surface area over all of right HG. Differences between right- and left-handers further demonstrates anatomical variability in the general population.

Studies investigating the link between HG morphology and function have found that the volume of HG gray (GM) and white (WM) matter may be more significant than the number of gyri. Wong et al. (2008) studied how quickly native English speakers could learn lexical tones and found the magnitude of learning success was related to greater HG GM and WM volumes in the left hemisphere but was independent of HG duplication. Decreased overall HG volume was correlated with less successful music pitch perception and less successful linguistic ability for tonal words (Wong et al., 2008). However, speech processing takes place in STG and the associative auditory cortex, such as PT. To explain the positive correlation between HG volume and successful learning of lexical tones, the authors suggest that, as a primary sensory structure, the HG may be important when learning unfamiliar acoustic speech signals. HG may be more actively recruited to process a word's basic auditory features when encountering and learning novel speech sounds.

Warrier et al. (2009) further explored how HG size related to the differential processing of acoustic information if it were presented temporally, similarly to language, or spectrally, similarly to music. Multiple structures and systems throughout the brain are recruited during the perception of music and language, but it is popularly accepted that music is processed predominantly in the right hemisphere, whereas the left hemisphere is principally responsible for language (Zatorre, 2003). Through fMRI BOLD imaging, Warrier et al. (2009) found bilateral activation along HG and PT in response to both types

of stimuli. However, activation was not equally significant in both hemispheres. Temporal information elicited greater activation in the left hemisphere showing a BOLD response around HG and posteriorly along STG. On the right, temporal information activated anterolateral regions of STG and posterolateral areas of the middle temporal gyrus (Warrier et al., 2009). Spectral information bilaterally activated areas of PT with greater activation on the right. Schneider et al. (2005) presented individuals with ambiguous tones, and individuals with right HG asymmetry showed preference to spectral information and those with left HG asymmetry showed preference to fundamental frequency. Warrier et al. (2009) suggest that variations in HG morphology may influence an individual's strategy when perceiving novel spectral acoustic signals. The ability to read depends on intact phonological processing and awareness which allows an individual to form, store, and manipulate mental representations of speech sounds. If differences in HG alter phonological processing strategies in the dyslexic brain, these structural differences may interfere with successful reading acquisition.

1.2.3 Review of HG in Specialized and Disordered Populations

The morphology of HG and PT have also been investigated in various specialized and disordered populations. Because the human PAC resides in HG, populations known for enhanced auditory skills (i.e., musicians and phoneticians) and those with disturbed (i.e., schizophrenics) auditory stimulation have been the main focus of such studies. Results from these studies have been analyzed to further understand how HG's structure may correlate with functional abilities and neural network connections.

1.2.3.1 Musicians

Several studies have investigated the role and influence of HG morphology and plasticity in musical ability and aptitude. One overall finding is that musical aptitude generally correlates with HG duplication patterns, HG size, and HG GM volume (Schneider et al., 2002). Specifically, rightward lateralization of HG is related to musical aptitude and pitch perception (Schneider et al, 2005; Wengenroth et al., 2014). Wengenroth et al. (2014) found that the gray matter volume in HG of the right hemisphere was correlated with the ability to perceive absolute pitch. Furthermore, the authors suggest that auditory networks of the right hemisphere may hold a base template crucial to pitch perception, while analogous structures of the left hemisphere are more important when integrating pitch perception with pitch labeling and pitch memory.

Benner et al. (2017) further investigated the patterns and magnitude of HG duplication in professional and amateur musicians and concluded that duplications of HG of any type are more common in musicians than in non-musical controls. 90% of the musician participants exhibited duplications of HG in one or both hemispheres, with 70% of total hemispheres containing multiple gyri with no significant difference in the frequency of occurrence between the left and right hemisphere. Benner et al. (2017) measured the amount of gyrification, or the number of transverse gyri and sulcal length, and found correlations between increase in gyrification with an increase in GM volume. In other words, configurations of HG duplications were found to contain increased GM volume compared to a single HG. The authors discussed that this increased HG gyrification and presence of multiple HG is innate to the brain of a musician and is not induced by years

of musical training and neuroplasticity. This suggests that the presence of multiple HG convey possible structural or connective advantages for musical aptitude.

Studies of HG duplication in musicians have also provided additional information about the potential function of additional HG. fMRI was used to investigate connectivity within and between HG with findings suggesting that additional gyri may form a single auditory unit with the most anterior HG (Benner et al., 2017). This contradicts the belief that the PAC resides solely in aHG and brings into question previous studies who have included secondary and tertiary HG as part of PT total volume. This "single unit" found in skilled musicians is supported by a previous study with control subjects which showed that the PAC spans several gyri in the configurations of HG duplications—the PAC was not restricted to the most anterior HG (Da Costa et al., 2011). Overall, these findings suggest that secondary HG may have more in common functionally with aHG than it does with PT.

1.2.3.2 Phoneticians

Phoneticians are known for their heightened acuity in identifying and discriminating speech sounds. Because of the relationship between HG, PT, and other structures in the language processing network, HG morphology in phoneticians has been studied and compared to controls. Results from these studies have shown that individuals who can more quickly perceive and learn new speech sounds demonstrate increased WM density and volume in their left HG, which results in a more pronounced left-lateralized temporal asymmetry (Golestani & Pallier, 2007; Golestani et al., 2007). While training of a skill like phonetic transcription can change the neurobiology of the brain through increased in white matter, duplication of HG and the number of gyri present may be innate

to an individual (Golestani et al., 2011). Consequently, this innate level of increased gyrification may bestow an individual with enhanced neural connections and brain volume which enhance the ability to learn and master advanced phonetics skills. Golestani et al. (2007) found that faster learners were more likely to display duplications of HG, and they proposed that this may predict anatomical differences in structures throughout the language network, specifically in structures responsible for rapid temporal processing. Furthermore, differences observed in the parietal lobe and right insula of faster learners is positively associated with differences in left HG morphology. Golestani and Pallier (2007) report associations between left HG WM volume with increased left-lateralized parietal lobe asymmetry and higher WM density in the insula, prefrontal cortex, and bilateral inferior parietal cortex in individuals who are better at learning new distinct speech sounds. While HG morphology may be associated with differences in auditory processing in other populations, these findings suggest that there are more global differences in brain anatomy, not solely duplications in HG, that affect aspects of language learning.

1.2.3.3 Schizophrenia

Studies of schizophrenic individuals have focused more on global and regional volumetric changes in brain anatomy, rather than specific configurations of gyral morphology. While the incidence and patterns of HG reduplication in schizophrenia have not been widely reported, studies of GM and WM volume changes in HG for this population can additionally inform how structural brain changes can influence functional impairment.

In schizophrenia, characteristic auditory hallucinations are accompanied by overall shrinkage of the temporal lobe. HG, located in the temporal lobe, is implicated in schizophrenia because it holds the PAC (Gaser et al., 2004). However, findings regarding the differences between HG volume in controls versus schizophrenics have been contradictory (Hirayasu et al, 2000; Smiley et al., 2013; Sumich et al., 2005; Yamasaki et al, 2007). Some studies have found a reduction in GM volume in the left and right HG of schizophrenics, while others have found no significant differences from control brains. Similarly, there have been opposing findings when investigating the connection between PT and delusional thoughts. Sumich et al. (2005) determined that delusional behavior was associated with an increase in left PT volume, with hallucinations and delusions correlated with a decrease in left HG volume. However, others have found reduction in PT volume in schizophrenic brains, in either the left (Hirayasu et al., 2000) or right (Yamasaki et al., 2007). There are overall brain changes in the temporal lobe and connected regions that correlate with hallucinations and delusional behavior in schizophrenia, but it is unclear the extent to which volume changes in HG are involved. The pathology of schizophrenia is likely caused by the interaction between abnormalities in several connected regions and not changes in HG or PT alone (Gaser et al., 2004). This might imply that variations in HG should not be the sole area of interest if the etiology of developmental dyslexia is to be fully understood.

1.3 Purpose of Current Study

The current project aimed to further investigate potential differences in HG morphology and GM volume between control and dyslexic brains and to determine if

increased GM volume or number of duplications is associated with the presence of a reading disorder. Previous studies which have investigated HG in dyslexia have been limited by small sample sizes, heterogeneous subject pools, and a lack of consensus on labeling protocol. First, we established a concise procedure for delineating HG morphotypes through structural landmarks (i.e., gyri and sulci). A prominent limitation of previous studies investigating HG configuration and size is the lack of consensus in defining label names, borders, morphotypes, and if HG2 belongs to the PAC or PT. Second, we determined if the attestation of various HG morphotypes differs significantly between dyslexic and control brains. Specifically, we investigated if reduplication of HG is more likely to occur in dyslexic brains and if there is a hemispheric preference for multiple gyri. Third, gray matter volume was measured for HG1, HG2, and total HG to investigate if the size of HG is different between dyslexic brains and controls and if reduplication affects gyral size. Studies of HG in controls have shown that HG reduplication occurs frequently in typically developing brains, including in individuals with aptitudes for phonetics and musical sounds (Benner et al., 2017; Golestani et al., 2007; Marie et al., 2015). Consistent with these results, we expected there to be no differences in the gyrification patterns of HG between control and dyslexic brains. Because we expected a similar proportion of morphotypes across control and dyslexic brains, we also expected that there would be no significant group differences in gray matter volume. However, consistent with most theories of left-lateralized language processing, we hypothesized that there would be increased gray matter volume in the left hemisphere compared to the right.

METHODS

2.1 Participants

Data included in this investigation were obtained from subjects previously recruited and consented for a study investigating variations in rapid neural adaptation between controls and individuals with dyslexia (Perrachione et al., 2016). These data were chosen to further explore what structural and morphometric variables may differ between the brains of controls and individuals with dyslexia. De-identified MRI data included scans from 33 control subjects and 34 dyslexic subjects. Subjects were all adult, native speakers of American English and free from any hearing, cognitive, or other speech and language impairments, per self-report. Subjects were balanced for age, sex, and years of education.

Subjects were identified as control or dyslexic through a battery of cognitive and behavioral language tests. The dyslexia battery included tests of phonology processing, rapid automatized naming, decoding of real- and non-words, and reading comprehension. A full description of tests and subtests is described in Perrachione et al. (2016) and its supplemental information. Performance on the timed and untimed tests of reading, specifically the WRMT-R/NU (Woodcock, 1998) subtests of Word Identification and Word Attack and TOWRE (Torgenson et al., 1999) subtests of Sight Word Reading and Decoding, were used to designate inclusion in the control or dyslexic study groups. Criteria for dyslexia was designated as performance at or below the 25th percentile on two or more of these subtests per test standardized norms. All subjects who met criteria for dyslexia also self-reported previously confirmed diagnoses of a reading disorder or a lifelong difficulty with reading.

Table 2.1. Subject demographics and behavioral scores. WRMT-R/NU: *Woodcock Reading Mastery Test -- Revised/Normative Update*, TOWRE: *Test of Word Reading Efficiency,* (*) denotes significant group mean difference $p < 0.05$, [a] chi-squared test, [b] unpaired Wilcoxon test

		Control (N=33)	Dyslexia (N=34)	Significance
	Sex (male/female)	16/17	9/25	0.107[a]
	Age (years)	22.0 ± 3.3	23.7 ± 5.4	0.361[b]
	Education (years)	15.3 ± 1.7	15.2 ± 2.0	0.885[b]
Test	**Subtest**	**Standard Score ± SD**		**Significance**
WRMT-R/NU	Word ID	110.4 ± 9.6	90.9 ± 8.9	0.000*[b]
	Word Attack	109.6 ± 14.1	89.3 ± 7.1	0.000*[b]
TOWRE	Sight Word Reading	108.7 ± 7.5	82.9 ± 10.9	0.000*[b]
	Decoding	108.2 ± 8.3	77.8 ± 9.9	0.000*[b]

2.2 Image Analysis

2.2.1 Classification of Heschl's Gyrus

The classification of gyrification patterns in each subjects' left and right hemispheres was completed according to the following criteria, based on previous described methods and neural landmarks by Marie et al. (2015) and Benner et al. (2017) (**Table 1.1**). HG is located in the superior temporal lobe and extends into the lateral fissure (Sylvian). HG was first identified by looking at pial surface-based cortical reconstructions obtained in FreeSurfer (v6.0.0) (http://surfer.nmr.mgh.harvard.edu/) (Dale et al., 1999) and cutting through the Sylvian fissure so that the superior surface of the superior temporal gyrus (STG) could be visualized. Once HG was preliminarily identified as a single gyrus, common-stem, complete, or multiple duplication in the surface, the morphotype was

confirmed by looking in the volume. HG was first identified in the sagittal plane and then confirmed in the coronal and axial planes (**Figure 2.1**).

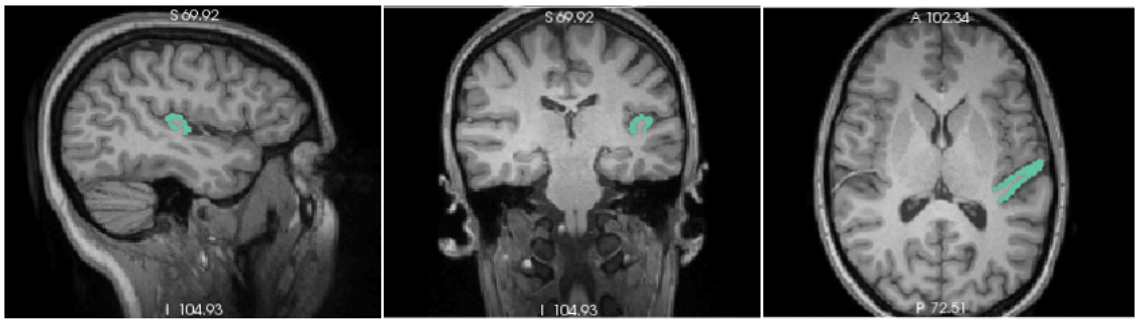

Figure 2.1. View of single Heschl's gyrus. HG is labeled in teal in the sagittal, coronal, and axial planes (*from left to right*). The characteristic Ω-shape can be seen in the sagittal and coronal planes.

There are several landmarks on the surface of STG that were used to determine HG morphotype (**Figure 2.2**). HG is bordered anteriorly by the first transverse sulcus (FTS) and posteriorly by Heschl's sulcus (HS) and PT. Common stem duplication (CSD) or partial reduplication were indicated by the presence of a sulcus intermedius (SI/SI of Beck) which divides HG laterally, extending at least one-third of the length of the gyrus, without reaching the medial border of the gyrus. In the case of a CSD, the terminus of HG2 was made at the medial end of the SI. The volume of the stem was included in the total volume of the anterior gyrus. Complete posterior duplication (CPD) or complete reduplication was indicated by the presence of a sulcus which extends laterally through HG to the medial border of the gyrus splitting the structure into anterior (HG1) and posterior (HG2) portions; this dividing crevice is the first Heschl's sulcus (HS1) with the second Heschl's sulcus (HS2) indicating the posterior border of HG2, separating HG from PT. Multiple duplications (MD) are characterized by the presence of multiple intermediate HS or combinations of CSD and CPD.

In both the sagittal and coronal planes, HG can be seen as an omega-shaped protrusion on the superior temporal gyrus (STG). The presence of a CSD will variably produce a heart shape and a CPD will variably produce an "m" shape. The look of MD structures will vary depending on the number of gyri and their configurations (**Figure 2.3**); most characteristically, MD can appear as distinct Z- and S- shapes, depending on their hemispheric location, in axial views (MD-Z, MD-S; Benner et al., 2017).

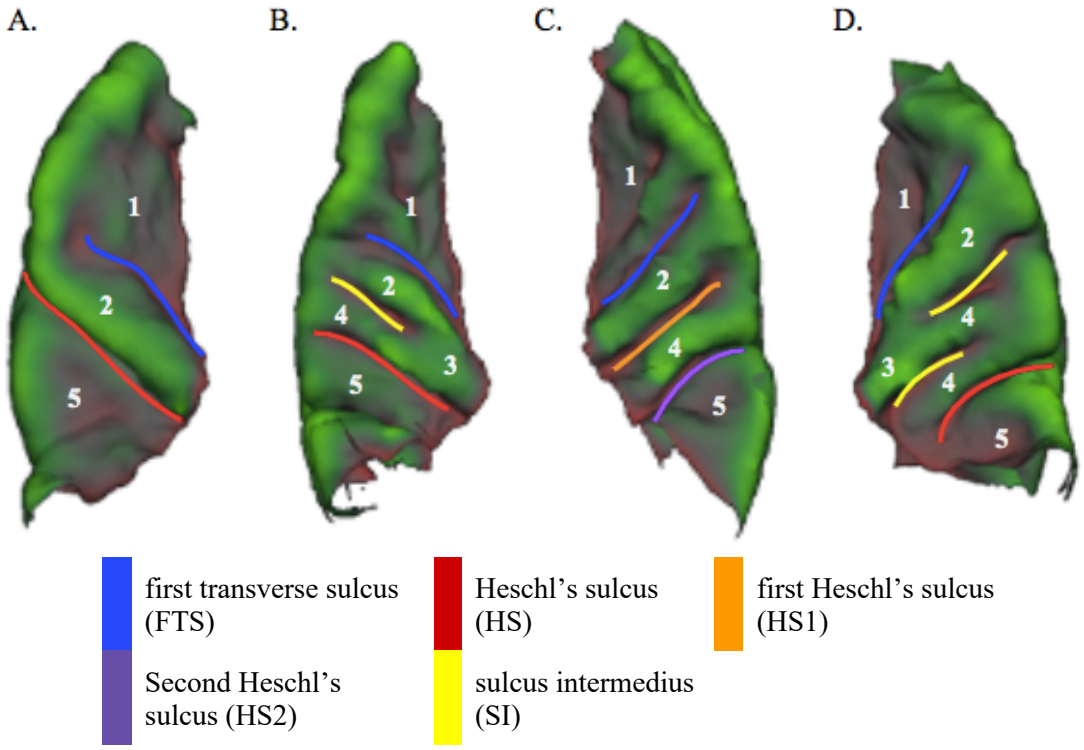

Figure 2.2. Identifying landmarks seen on the pial surface of the superior temporal plane. A: single Heschl's gyrus (SH), B: common stem duplication (CSD), C: complete posterior duplication (CPD), D: multiple duplication (MD-S); 1: planum polare, 2: first/anterior Heschl's gyrus (HG1), 3: common stem, 4: second/posterior Heschl's gyrus (HG2), 5: planum temporale (PT).

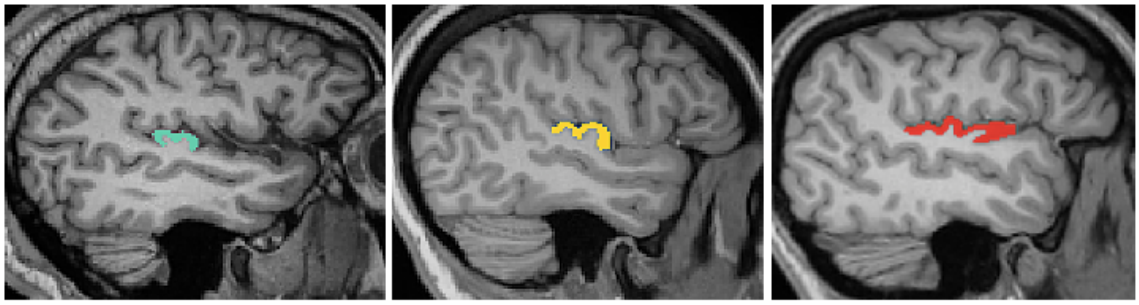

Figure 2.3. Appearance of HG in sagittal planes. The characteristic shapes of HG morphotypes can be in the sagittal plane. CSD appears as a heart-shape, CPD looks like the lowercase letter "m," and MD shows multiple protrusions (*from left to right*).

2.2.2 Labels & Volume Measurements

MRI data were analyzed using FreeSurfer (v6.0) software and its *tksurfer* and *FreeView* visualization tools. Each subject's original MR data were analyzed by a primary rater (JAC) to assign the HG morphotype (SH, CSD, CPD, or MD) in each hemisphere. The primary rater was blinded to the group assignment (control or dyslexic) of each subject. HG morphotypes were confirmed by three additional raters. After consensus was reached, labels were drawn on the inflated surface of each brain scan. These surface labels were then converted into the MRI volume and manually edited. The final structure volume was determined by obtaining the total number of voxels included within each volume label (1 voxel = $1mm^3$).

Surface labels were manually drawn using the visualization tool *tksurfer* included in FreeSurfer. Inflated brain surfaces were used to more accurately identify the gyri and sulci of interest because macroanatomical features are more clearly seen "on surface based representations and not on slices" (Ghosh et al., 2010, p. 87). Surface labels were drawn according to guidelines outlined below. Examples of complete surface labels for each of the HG morphotypes can be seen in **Figure 2.4**. Surface labels were then converted to

labelled volume using the algorithm in *mri_label2vol*. Volume labels were then edited using the software *FreeView* to correct any errors created or data omitted during surface-to-volume transformations. These errors included voxels outside the surface or outside the regions of HG, omitted voxels within the regions of HG, and voxels that overlapped between labels. Errors were corrected by manually adding or deleting individual voxels. MR scans of each subject were viewed slice by slice in sagittal, coronal, and axial planes to ensure labels were continuous and within the defined borders of HG.

Single Heschl's Gyrus (SH)

SH labels were drawn by following FTS and HS. Label limits extended from the complete medial end of the gyrus and terminated laterally where HG met STG.

Common Stem Duplication (CSD)

CSD labels were divided into three sections: a-hg, p-hg, and hg-stem. The CSD stem, hg-stem, was designated by identifying the medial point of the sulcus intermedius (SI) and drawing a line perpendicularly across the width of HG. This line separated the stem from the two gyral legs of the CSD morphotype. The perimeter of hg-stem was drawn by following FTS and HS and connecting with the line through SI. The anterior gyrus, a-hg, was labeled by connecting to hg-stem and tracing along FTS and SI. The posterior gyrus, p-hg, was labeled by connecting to hg-stem and tracing along SI and HS. Both a-hg and p-hg labels terminated laterally where HG met STG. In volumetric analysis, the hg-stem and a-hg labels were combined as HG1 (total).

Complete Posterior Duplication (CPD)

CPD labels were divided into two sections: a-hg and p-hg. The anterior gyrus, a-hg, was designated by tracing along FTS and HS1, which divides the two legs of CPD morphotypes. The posterior gyrus, p-hg, was marked by tracing along HS1 and HS2, which divides HG from PT. Both labels extended completely to the medial ends of each gyrus and terminated laterally where the gyri met STG. In volumetric analysis, a-hg labels designated HG1 and p-hg labels designated HG2.

Multiple Duplications (MD)

MD labels were drawn similarly to CSD and CPD configurations. The most anterior gyrus was labeled a-hg. In MD-S and MD-Z configurations, hg-stem was traced in accordance with CSD labels and combined with a-hg to create HG1 for volumetric analyses. p-hg included all gyri posterior to SI (in MD-S and -Z variants) or HS2 (in CSD/CPD combination variants). p-hg was separated from PT by HS2. For volumetric analyses, p-hg labels designated HG2.

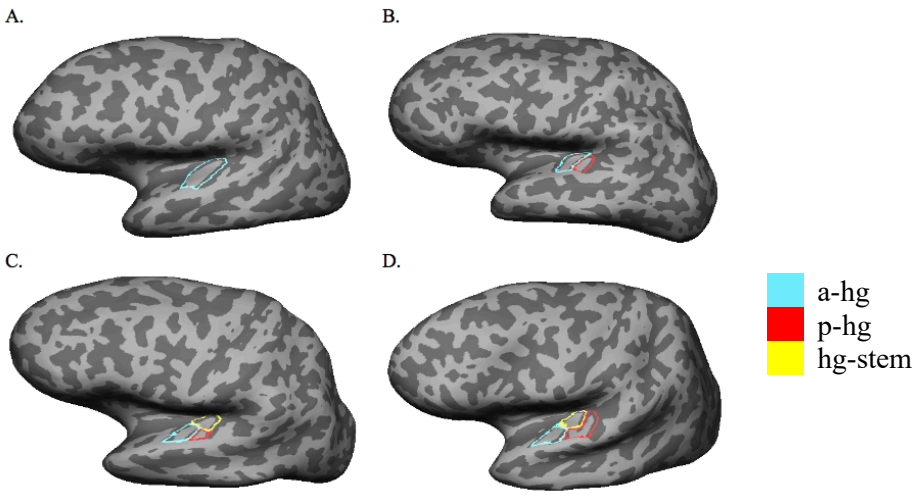

Figure 2.4. Outlines of surface labels. A: single Heschl's gyrus (SH), B: complete posterior duplication (CPD), C: common stem duplication (CSD), D: multiple duplication – Z-configuration (MD-Z).

2.2.3 Data Analysis

All analyses were completed using R (v3.6.3) and were implemented with *lmer*, *ez,* and *dplyr* packages.

2.2.3.1 Distribution of HG Morphotypes

Chi-squared tests were performed to identify if there was any significant difference between the incidence of HG duplication between control and dyslexic subjects, if HG duplication patterns differed between hemispheres, and if interhemispheric duplication patterns differed between groups. The types of HG duplication patterns were investigated in two different modes. First, all four morphotypes were considered and analysis of type contained four levels (*type:* SH, CSD, CPD, and MD). Next, all duplicated morphotypes were combined and analysis of type contained two levels (*typeSimple:* single and duplicated). This allowed us to separately investigate the frequency of all HG morphotypes and the incidence of duplication overall.

2.2.3.2 HG Gray Matter Volume

We compared total HG volume between both groups to examine *group* (control vs. dyslexic), *hemisphere* (left vs. right), and *type/typeSimple* interactions. HG1 volume was analyzed to see if duplication pattern had any effect on HG1 size. This allowed us to investigate whether HG reduplicates at the expense of HG1 volume. Finally, we examined if HG volume is lateralized in dyslexic brains and if that pattern of asymmetry is different from the control group.

For volume analyses, we used a linear mixed-effects model and Type III analyses of variance (ANOVAs), with random effects for participants. The volumes of individual

structures or total HG volume were the dependent variables, and fixed effects included group, hemisphere, and HG morphotype. The more flexible linear mixed model was used to account for multiple variables within subjects, including information from left and right hemispheres of the same brain. Statistical significance of effects was determined by a p-value of < 0.05, with degrees of freedom estimated via the Satterthwaite method.

The interhemispheric asymmetry of HG volumes were calculated using the formula $(V_L - V_R)/[0.5 * (V_L + V_R)]$ – where V is volume and L and R are the left- and right-hemisphere structures, respectively – as described by Smiley et al. (2009) in a study comparing altered volume and patterns of asymmetry between controls and schizophrenic brains. A positive value signified leftward asymmetry and a negative value corresponded to rightward asymmetry. A chi-squared test was used to compare the proportions of left- and right-lateralized brains in each group. To compare the degree of asymmetry in each group, a Shapiro-Wilk test was used to assess if the asymmetry indices followed a normal distribution and a t-test was used to compare the group means with a p-value of < 0.05 indicating statistical significance.

RESULTS

3.1 Distribution of Morphotypes

Examination of HG morphotypes between groups showed a significant effect ($\chi^2(3, 67) = 8.74$, $p = 0.033$) of *type* when accounting for all four possible morphotypes, but no significant effect of type when considering simple single vs. duplicated HG morphotypes ($\chi^2(1, 67) = 0$, $p = 1$). MD morphotypes seem to occur more frequently in dyslexic brains (**Figure 3.1**); of the 11 MD identified, 10 (91%) were found in dyslexic brains while only 1 (9%) was observed in controls. When looking at reduplication in general, duplication of HG occurred at a similar proportion in control and dyslexic brains (**Figure 3.2**). Additionally, there was no difference in the proportion of HG morphotypes between the left and right hemispheres in controls ($\chi^2(3, 33) = 1.82$, $p = 0.610$) or in dyslexics ($\chi^2(3, 34) = 2.45$, $p = 0.484$). It follows that there was also no significant difference in the occurrence of left and right hemisphere duplications between control ($\chi^2(1, 33) = 0.251$, $p = 0.617$) and dyslexics ($\chi^2(1, 34) = 0$, $p = 1$). This suggests that one morphotype does not occur more frequently in one hemisphere than the other in either group. Left HG configuration did not differ between controls and dyslexics, ($\chi^2(3, 67) = 3.24$, $p = 0.356$; $\chi^2(1, 67) = 0.123$, p = 0.725). In the right hemisphere, the greater proportion of MD in dyslexic brains approached significance ($\chi^2(3, 67) = 6.71$, $p = 0.0818$), but right HG duplications overall did not differ between groups ($\chi^2(1, 67) = 0.0235$, $p = 0.878$). These results overall suggest that no one HG morphotype occurs more frequently in either the left or right hemispheres, nor is the incidence of HG duplication in dyslexic brains significantly different from controls. There was limited evidence for disproportional attestation of the MD morphotype in the right hemisphere of dyslexic brains; however, the overall rarity of this particular morphotype

means we may not have had sufficient statistical power to detect group differences in MD prevalence or lateralization.

Table 3.1. Distribution of HG morphotypes by hemisphere for each study group. The most frequently occurring morphotype was SH, but HG reduplication was common in both groups. MD at a much higher frequency in dyslexic brains

	Single gyrus			Common stem duplication			Complete posterior duplication			Multiple duplications		
	lh	*rh*	*total*	*lh*	*rh*	*total*	*lh*	*rh*	*total*	*lh*	*rh*	*total*
Control (N = 66)	15	12	27 (40.9%)	9	8	17 (25.8%)	9	12	21 (31.8%)	0	1	1 (1.5%)
Dyslexia (N = 68)	13	14	27 (39.7%)	10	7	17 (25%)	8	6	14 (20.6%)	3	7	10 (14.7%)

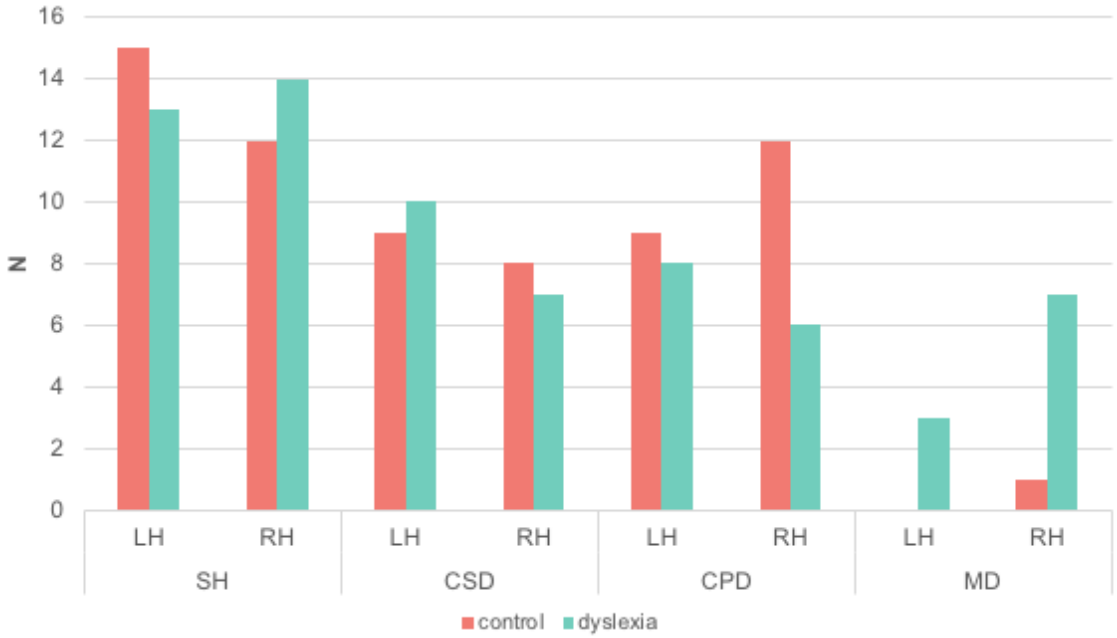

Figure 3.1. Distribution of HG morphotypes in control and dyslexic brains. All HG morphotypes occurred in similar frequency for both groups across hemispheres, except for MD. MD occurred more frequently in dyslexic brains in the right hemisphere.

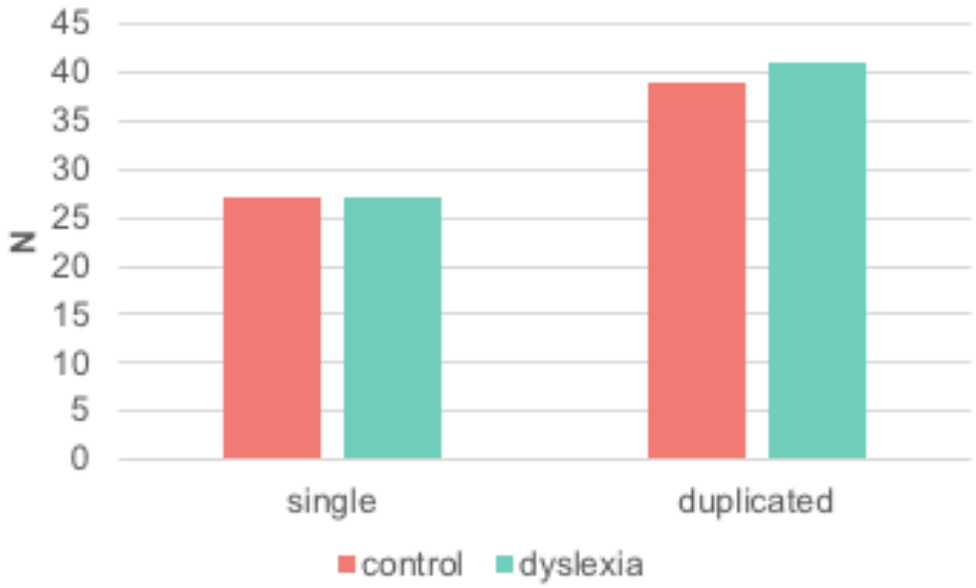

Figure 3.2. Distribution of single and reduplicated gyri in control and dyslexic brains. HG reduplication was just as likely to occur in controls as individuals with dyslexia.

When all morphotypes across groups were examined, bilateral SH was the most common pattern seen in individuals (**Figure 3.3**, **Table 3.2**). However, when the presence of a single gyrus or duplication was considered, some interesting patterns were observed. It appeared that if a single gyrus was present in the left hemisphere of an individual, a single or duplication were equally likely to be observed in the right hemisphere. However, when a duplication was present in the left hemisphere of an individual, a duplication in the right hemisphere appeared more likely to occur than a single gyrus (**Figure 3.3**, **Table 3.3**). A larger sample size is needed to explore the significance of these contingencies and to understand if there is a relationship between interhemispheric duplication.

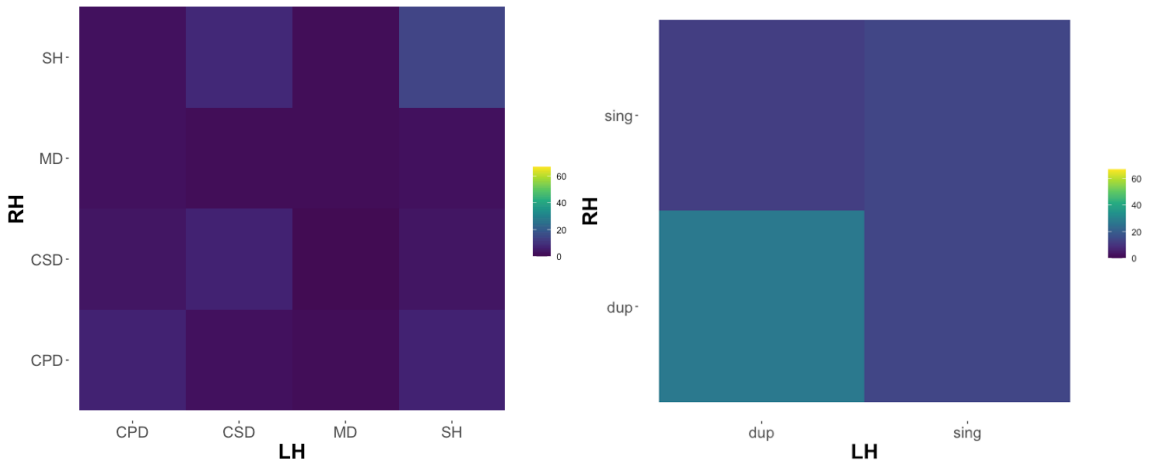

Figure 3.3. Distribution of HG duplication patterns across hemispheres for all subjects. Distribution frequency of all four morphotypes shows bilateral SH is the most common HG pattern (*left*). If patterns of HG reduplication are simplified as "single (sing.)" and "duplicated (dup.)" bilateral duplication occurs most frequently while other patterns occur at approximately the same frequency (*right*).

Table 3.2. Number and percentage of interhemispheric HG patterns by morphotype

Left Type, N (%) \ Right Type, N (%)	**SH**	**CSD**	**CPD**	**MD**
SH	14 (21%)	4 (6%)	7 (10%)	3 (4.5%)
CSD	8 (12%)	7 (10%)	3 (4.4%)	1 (1.5%)
CPD	3 (4.5%)	4 (6%)	7 (10%)	3 (4.5%)
MD	1 (1.5%)	0 (0%)	1 (1.5%)	1 (1.5%)

Table 3.3. Number and percentage of interhemispheric HG patterns as "single" or "duplicated."

Left TypeSimple, N(%) \ Right TypeSimple, N(%)	**Single**	**Duplicated**
Single	14 (21%)	14 (21%)
Duplicated	12 (18%)	27 (40%)

3.2 HG Gray Matter Volume

3.2.1 Total HG Volume

Between controls and dyslexic brains, there was a significant effect for *group* ($F(1, 65) = 4.30$, $p = 0.042$) with individuals with dyslexia showing a slightly larger total HG volume overall (**Figure 3.4**). There were no significant effects between *hemispheres* or in *group* × *hemisphere* interactions. *Type* showed a significant effect on total HG volume ($F(3,118) = 24.7$, $p = 0.000$), with a much larger total volume seen in HG with MD configurations (**Figure 3.6**). There was no significant effect seen in *hemisphere* × *type* interactions. Because MD were observed more often in dyslexic brains, a secondary analysis which excluded all MD was performed to test if MD volume was driving the significant *group* effect. Omitting MD morphotypes removed the significant effect for *group* ($F(1, 54) = 1.19$, $p = 0.281$) (**Figure 3.5**). There was a significant effect of *typeSimple* on total HG volume ($F(1, 118) = 70.9$, $p = 0.000$) and a significant effect of *hemisphere* × *typeSimple* interactions ($F(1, 93) = 6.63$, $p = 0.012$). Duplication resulted in a total HG volume which was significantly greater than a single gyrus. This was true across the left and right hemispheres. However, when there was a single gyrus in the right hemisphere, its volume was significantly smaller than when there was a single gyrus on the left (**Figure 3.7**). This effect was still significant after removing MD from the analysis ($F(1, 108) = 54.4$, $p = 0.000$).

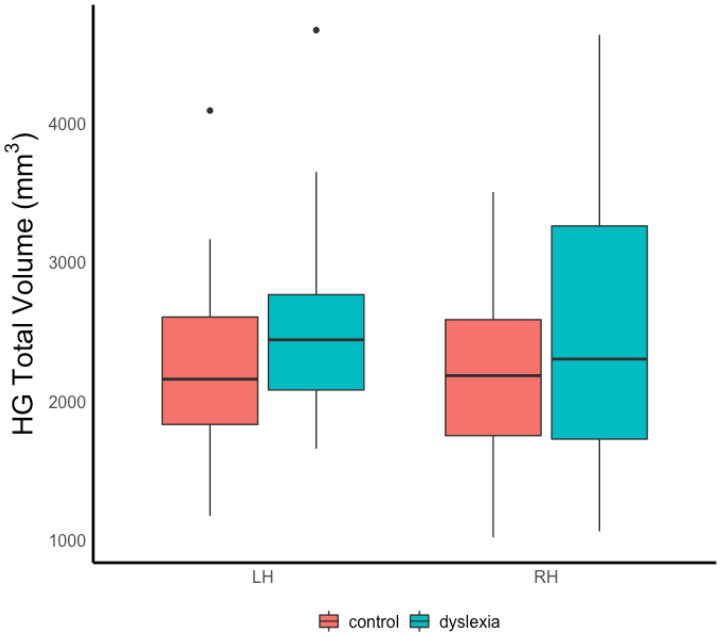

Figure 3.4. Total HG volume across group and hemisphere. On average, total HG volume is larger in dyslexic brains compared to controls.

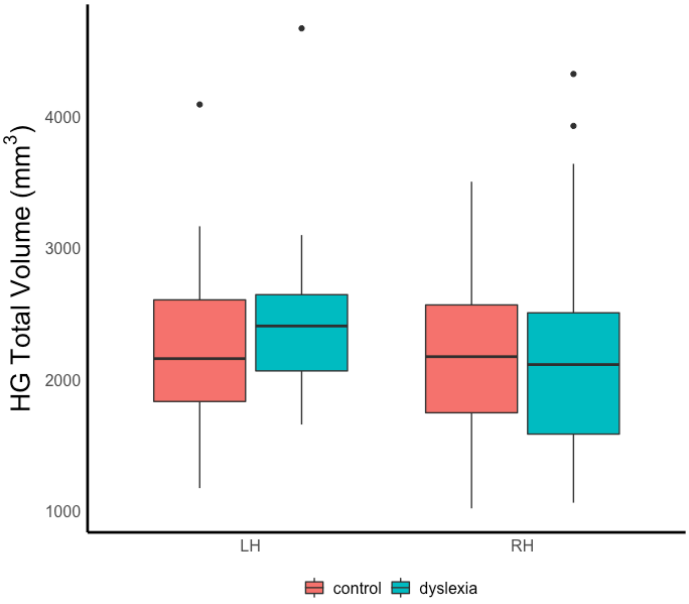

Figure 3.5. Total HG volume across group and hemisphere excluding MD. When the MD morphotype was excluded from the analysis, the significant difference in total HG volume between groups disappeared.

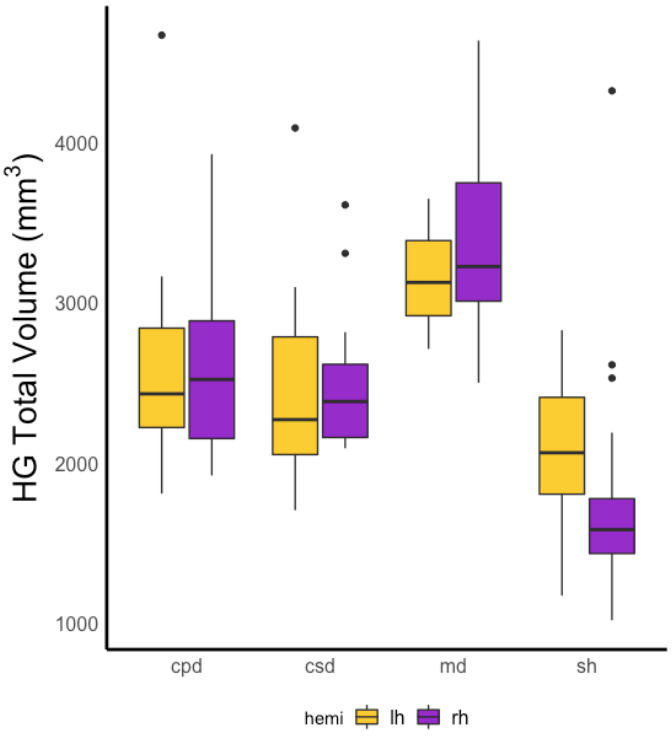

Figure 3.6. Total HG volume in each morphotype across hemispheres. On average, the total HG volume of the MD morphotype is significantly larger than the other morphotypes.

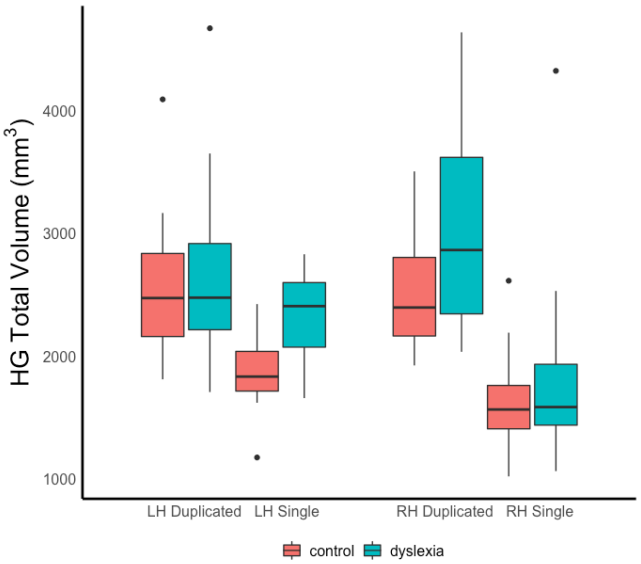

Figure 3.7. Total HG volume in "single" and "duplicated" across hemisphere and group. HG duplication resulted in greater total HG volume across the left and right hemispheres. Single gyri were significantly smaller in the right hemisphere compared to the left in both groups.

3.2.2 First and Second Heschl's Gyri Volumes

There was a significant effect of *hemisphere* on HG1 volume ($F(1, 65) = 9.47$, $p = 0.04$) with larger HG1 volumes in the left hemispheres of both control and dyslexic brains (**Figure 3.8**). Due to its overall rarity and the lack of MD morphotypes in controls in particular, analysis of the *type* factor is precluded. Thus, *typeSimple* was analyzed. There were significant effects of *group* ($F(1, 62) = 4.50$, $p = 0.038$) and *hemisphere* ($F(1, 60) = 11.51$, $p = 0.001$), but no *group* × *hemisphere* interaction ($F(1, 60) = 0.003$, $p = 0.957$) (**Figure 3.9**). When just looking across groups, HG1 volume in dyslexia was larger than in controls. When just looking across hemispheres, HG1 volume was greater in the left hemisphere. If MD were removed from the analysis, the significant effect of *group* was reduced ($F(1, 60) = 3.76$, $p = 0.057$), but did not disappear altogether (**Figure 3.10**). This suggests that HG1 volume is overall larger in MD morphotypes, but a larger sample of MD would need to be studied for more conclusive answers. Additionally, there was no significant effect of *typeSimple* on HG1 volume, which implies that HG1 volume is not significantly affected by reduplication. However, this may suggest that additional HG gyri may negatively affect PT volumes – a question for future research.

There was a significant effect of *hemisphere* on HG2 volume ($F(1, 35) = 8.88$, $p = 0.005$) (**Figure 3.11)**. If HG2 volume in each morphotype is examined, there is a strong effect of *type* on HG2 volume ($F(2, 68) = 33.1$, $p < 0.0001$). However, analysis by *type* is under-powered due to rare attestation of the MD type and should be considered with caution. This significance is likely due to the individual and combined effects of a much smaller HG2 volume in CSD morphotypes and a much larger HG2 in MD morphotypes.

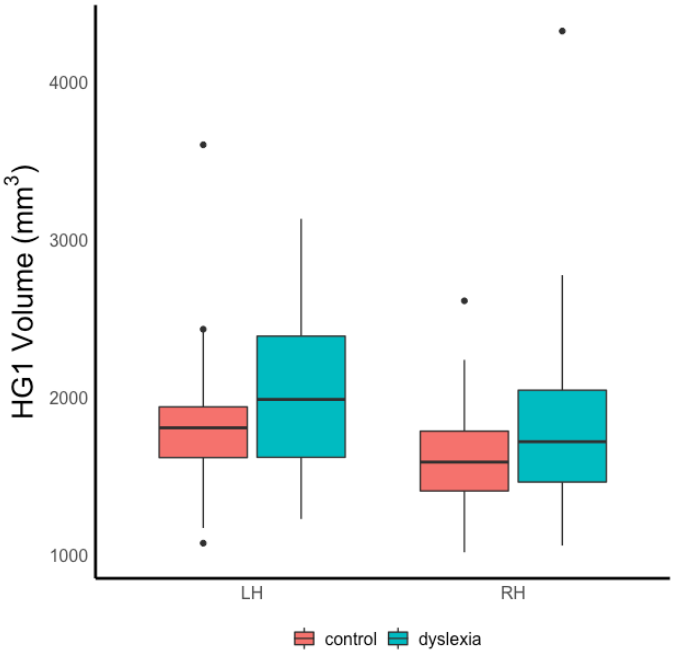

Figure 3.8. HG1 volume across group and hemisphere. In both control and dyslexic brains, the volume of HG1 was slightly larger in the left hemisphere.

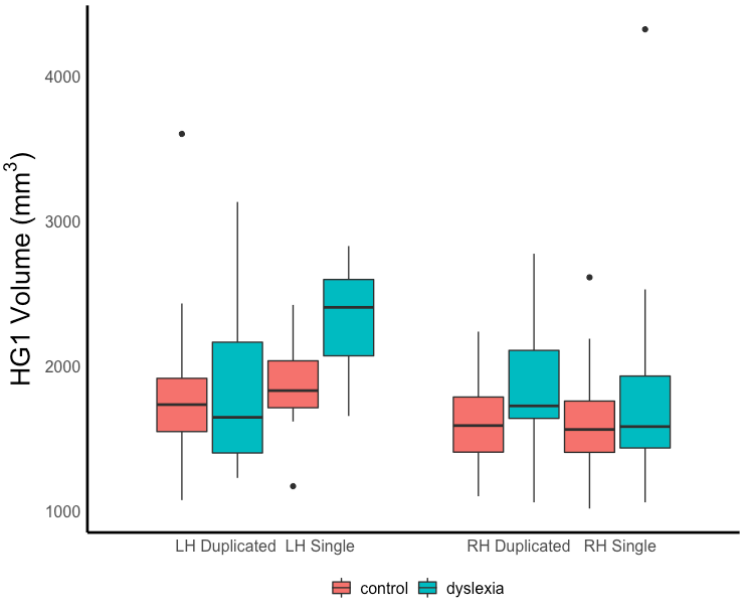

Figure 3.9. HG1 volume in "single" and "duplicated" across group and hemisphere. When considering group, the volume of HG1 was greater in dyslexic brains than in controls. When considering hemisphere, the volume of HG1 volume was greater in the left hemisphere.

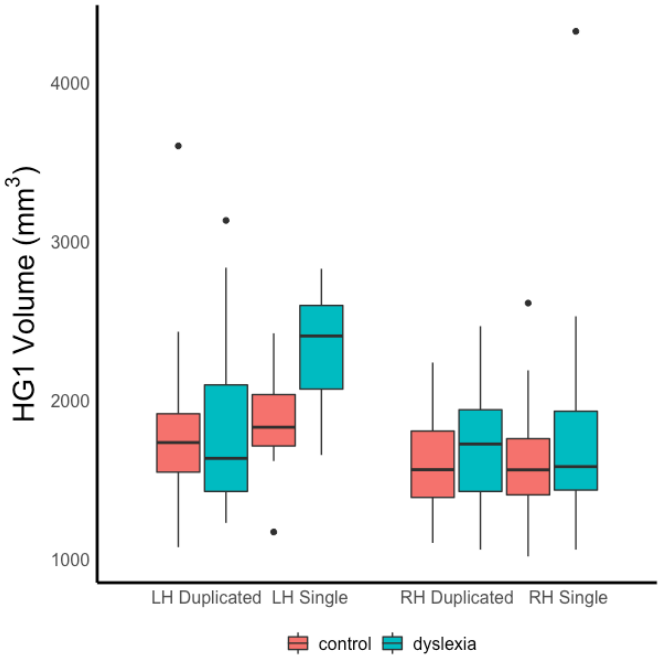

Figure 3.10. HG1 volume in "single" and "duplicated" across group and hemisphere excluding MD. If the MD morphotype is excluded, "duplicated" HG1 volume in the right hemisphere is slightly larger in dyslexic brains than in controls. Because most of the observed MD were in the right hemisphere, left HG1 volume analyses were not significantly affected.

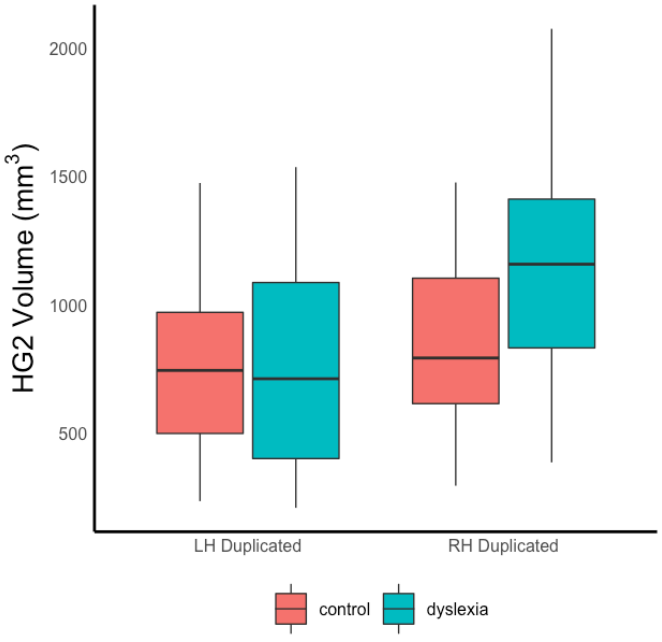

Figure 3.11. HG2 volume across group and hemisphere. The volume of HG2 is greater in the right hemisphere in both control and dyslexic brains.

3.2.3 Hemispheric HG Asymmetry

There was no significant difference in the proportion of left-lateralized versus right-lateralized brains between groups ($\chi^2(1, 67) = 0$, p = 1) (**Table 3.4**). Dyslexic brains showed the same prevalence of leftward HG asymmetry as controls. Overall, 54% all brains combined showed leftward HG asymmetry and 46% showed rightward HG asymmetry ($\chi^2(1, 67) = 0.373$, p = 0.541), These results contrast with the typically observed leftward lateralization of language structures in the brain. This suggests that total HG volumes alone may not be a reliable marker of how volume is distributed throughout the brain to support language processing and production. Mean asymmetry indices (AI) between control and dyslexic brains were also not significantly different ($t(65) = 0.025$, $p = 0.980$) (**Table 3.5**). Additionally, mean AI for both groups were relatively small. This suggests that, overall, total HG volume is not prominently lateralized to one hemisphere. However, if only HG1 volume was considered, there was a higher incidence of leftward asymmetry (72%) compared to rightward asymmetry (28%) ($\chi^2(1, 67) = 12.6$, p = 0.0003) (**Figure 3.12**). This result correlates with significantly larger HG1 volumes observed in the left hemisphere. The leftward lateralization of HG1 also corresponds to previous investigations of aHG which found larger HG in the left hemisphere compared to the right (Marie et al., 2015). Both groups showed similar proportions of hemispheric lateralization for HG1 ($\chi^2(1, 67) = 0$, p = 1) (**Table 3.4**), and mean AI for HG1 was also not significantly different between groups ($t(65) = 0.246$, $p = 0.807$) (**Table 3.5**). Overall, this result suggests that HG1 is left-lateralized to a similar degree in control and dyslexic brains.

Table 3.4. HG lateralization across groups. In both control and dyslexic brains, total HG was not significantly lateralized to the left or right hemispheres, but HG1 was more often lateralized to the left hemisphere.

	Total HG		HG1 only	
	Left-lateralized	*Right-lateralized*	*Left-lateralized*	*Right-lateralized*
Control	18	15	24	9
Dyslexia	18	16	24	10

Table 3.5. Mean Asymmetry Index (AI). In both control and dyslexic brains, total HG volume did not significantly differ between hemispheres, and the magnitude of HG1 lateralization was similar.

		Mean AI (SD)	
	N	*Total HG*	*HG1 only*
Control	33	0.0438 (0.338)	0.120 (0.263)
Dyslexia	34	0.0416 (0.376)	0.104 (0.247)

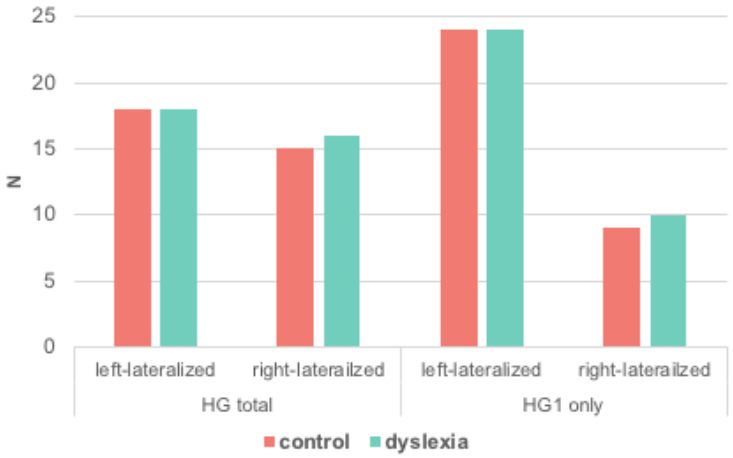

Figure 3.12. Hemispheric lateralization in HG. Total HG was not significantly lateralized to the left or right hemispheres in either group. However, HG1 was significantly left-lateralized in both control and dyslexic brains.

DISCUSSION

4.1 Summary of Results and Clinical Applications

One reason to better understand structural differences between disordered and typical brains is that anatomical abnormalities can add predictive power to the results of behavioral testing. By understanding how dyslexic and control brains differ, we may be able to predict reading disorders earlier and with more accuracy. This will lead to the earlier implementation of therapeutic interventions. Additionally, a better understanding of the disrupted structural and functional differences in dyslexia may allow for the development of more targeted treatments and more specific compensatory strategies.

Analysis of HG morphotype frequency suggests that patterns of HG reduplication do not significantly differ between typical readers and those with a developmental reading disorder. MD configurations appear to occur more frequently in dyslexic brains. However, there was a limited total number of MD overall. MD is a very rare morphotype, but a more conclusive pattern connecting the MD morphotype with dyslexia could develop with a larger sample size. Looking at the incidence of HG reduplication in general, our results show that duplication occurs just as frequently in controls as in dyslexic brains. The high proportion of duplication in the hemispheres of control brains (~59%) corresponds with previous studies of HG morphology in healthy controls. For instance, Marie et al. (2015) found that duplication occurred in one or both hemispheres 64% of the time in right-handers and 51% of the time in left-handers. Interhemispheric duplication in dyslexic brains occurred at a similar frequency (~60%). Warrier et al. (2009) suggest that this high degree of variability in HG may be reflective of normal inherent differences in the processing of acoustic information between individuals. Overall, our findings suggest that

HG duplication alone is not a distinguishing feature in dyslexic brains. Leonard et al. (2001) listed four anatomical and morphometric risk factors for dyslexia, including HG reduplication. It is possible that HG duplication is related to behavioral symptoms of dyslexia, but only if reduplication occurs in the presence of other structural neural abnormalities.

Reading is a complex process which requires the coordination of several systems, including auditory, language, visual, and attentional (Norton et al., 2015). It is unlikely that reading impairments develop from a single structural abnormality, such as HG reduplication, but instead arise from a cumulative effect of multiple systemic impairments. In addition to macroanatomical differences, impairments in rapid neural adaptation, grapheme-to-phoneme mapping (long segment of the arcuate fasciculus), and the visual word form area (inferior fronto-occipital fascicle) have been identified in the dyslexic brain (Kraft et al., 2016; Perrachione et al., 2016). Furthermore, in the brains of phoneticians and musicians, an increase in the number of gyri and gyral volume gave these individuals a functional advantage (Benner et al., 2017; Golestani et al., 2011). Thus, HG duplications may only convey disadvantage in the presence of overall abnormal brain development. To better understand if HG duplication can affect reading skills, the structural and functional differences of all structures, including HG, in the language networks of the dyslexic brain need to be further studied.

While HG morphotypes were similar between control and dyslexic brains, there were differences in HG volumes between the two groups. HG, overall, was larger in dyslexic brains than in controls. However, this significance might only be driven by the

larger number of MD observed in dyslexic brains. In both control and dyslexic brains, the MD led to an increase in HG volume. Because most MD were in dyslexic brains, the effect from MD may have only shown significance in those brains, giving the illusion that HG has more gray matter volume in dyslexic brains. When MD were excluded from this analysis, total HG volume in both groups was about the same. A larger sample size could elucidate this effect and confirm if MD does occur more frequently in dyslexic brains and increase total HG volume. Interestingly, when all subjects were considered, HG1 volume was significantly greater in dyslexic brains. With MD morphotypes removed from the analysis, the difference in HG1 volume between dyslexic and controls brains approached significance. This may suggest that while reduplicated HG are not distinctive of dyslexic brains, larger GM volume of HG1 is. HG1 volumes were greater overall in the left hemisphere in both groups which may be related to the innate leftward asymmetry of the temporal lobe seen in language networks of the general population. Indeed, when hemispheric asymmetry was judged by HG1 volume alone, both groups showed a higher proportion of leftward lateralization. It has been speculated that this may relate to the greater role of left HG in the processing of temporal acoustic information compared to the role of right HG in the processing of spectral acoustic signals (Marie et al., 2015). Differences in HG2 volumes across hemispheres were likely driven by the higher incidence of MD in the right and the significantly smaller second gyral arm in CSD configurations. However, without further understanding about the functional connectivity of HG2 and whether primary auditory or associative neurons are contained within its gray matter

volume, it is difficult to determine if the size of HG2 conveys a significant effect on hearing or language.

4.2 Considerations for the Labeling Protocol Adopted for this Study

One purpose of this investigation was to create a more specific and less biased protocol for delineating Heschl's gyri and PT. As previously reviewed (**Table 1.1**), there has been a wide variation in the criteria for labeling HG and PT between studies. Thus, it has been difficult to draw accurate conclusions about the size of HG and PT from the results of these studies. Our protocol sought to label HG solely on structural characteristics. First HG (HG1) was positioned between the first transverse sulcus and Heschl's sulcus (HS). In the case of reduplication, HG1 was bordered posteriorly by sulcus intermedius (SI) or first Heschl's sulcus (HS1). HG2 was set between SI or HS1 and second Heschl's sulcus (HS2). Typically, the primary difference between HS1 and HS2 is that HS2 laterally splits STG. However, there was wide morphological variability between brains and even these distinct landmarks created ambiguity and required subjective judgment.

The boundary between HG1 and HG2 was indistinct at times. There were some incidences of a SI with an "o" configuration where both gyri remained connected medially and laterally with a shallow sulcus between them (**Figure 4.1**). When viewed in the sagittal plane of the volume, the characteristic heart-shape of a CSD could be seen. In some cases, HG1 and HG2 were clearly separated laterally and medially, but were conjoined by a small isthmus reflected in an "x" configuration in HS1 (**Figure 4.2**). In the sagittal planes, these gyri formed the characteristic "m" shape of a CPD. These were, thus, treated as CPD and divided by following HS1 and cutting through the connecting segment.

Figure 4.1. Sulcus intermedius "o" configuration. The "o" configuration is formed when HG1 and HG2 connect at the medial end, forming a minimal stem.

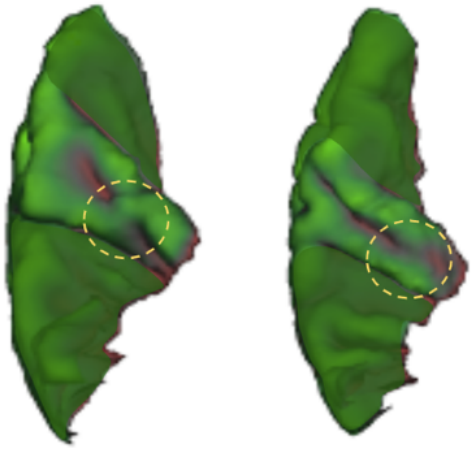

Figure 4.2. First Heschl's sulcus "x" configuration. The "x" configuration is formed when HG1 and HG2 briefly connect in the middle and then separate completely at the medial end.

In the majority of cases, the most confounding boundary to identify was where HG2 ended and PT began. In line with our labeling scheme, a convolution was designated as HG2 if there was a distinct second gyrus. However, the curvature of HG2 varied widely, and we questioned if less steep gyri were actually just planar variation in PT (**Figure 4.3**). There were some instances where HG2 was located more posteriorly to HG1 than expected. This led to a larger apparent surface area and more planar appearance in HG2 (**Figure 4.3**). The designation of HG2 was further confounded by a surprisingly regular variability in the curvature of PT. PT is so named for its flat appearance; however, pial surface representations revealed several maxima and minima within PT (**Figure 4.4**). To prevent inaccurate labeling of HG2, HG was compared between surface- and volume-based representations. Ambiguous HG2 seen in a surface could be confirmed as more distinct protrusions or flat regions in a volume. This highlights the importance of using multiple

and simultaneous views of a brain when labeling anatomical structures in order to label them accurately.

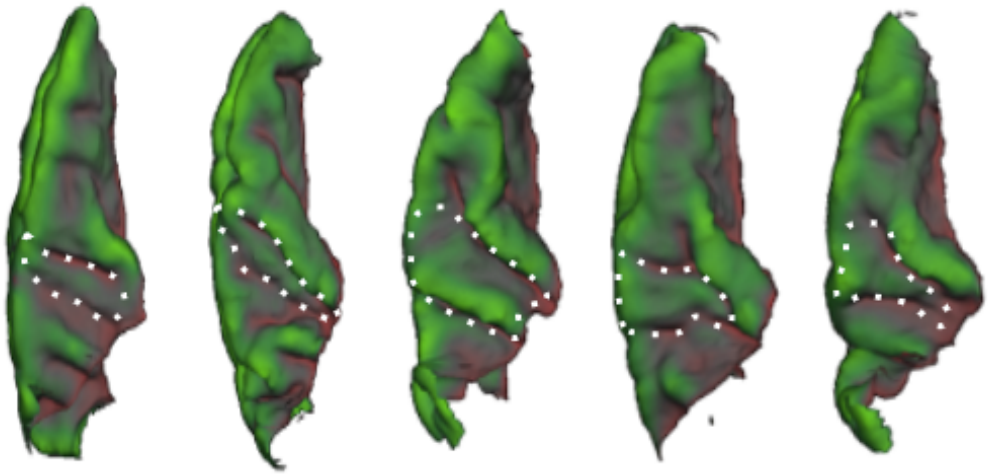

Figure 4.3∫. **Morphological variability of HG2 in surface representations.** Second Heschl's gyrus, outlined in white, ranges in its width and the steepness of its curvature.

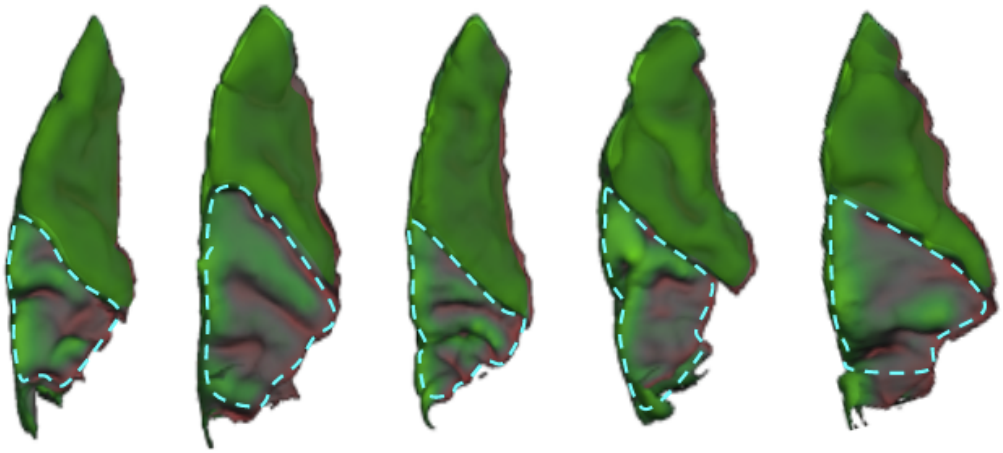

Figure 4.4. Morphological variability of PT in surface representations. The surface of planum temporale, outlined in blue, varies from highly convoluted (*left*) to planar (*right*).

Finally, there is a high amount of variability in the appearance of the MD morphotype (Figure 4.5). Because this is a rare morphotype, it is unknown if one pattern is more likely to occur (e.g., S-shape vs. Z-shape), and if this has a functional effect on

HG1. The appearance of PT is also variably affected by multiple reduplications. In some MD, PT appears non-existent. Overall, this is an interesting morphotype and may deserve more recognition in future morphological studies of HG and PT.

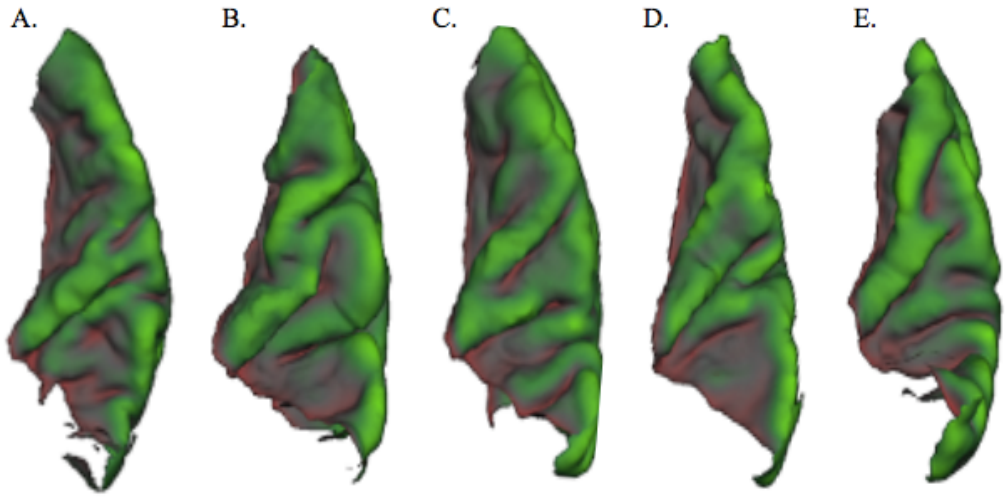

Figure 4.5. Morphological variability of MD in surface representations. A: S-shape with a prominent common stem; B: S-shape with a common stem; C: S-shape with minimal common stem; D: Z-shape; E: combination of two CSD morphotypes.

Despite the high degree of variability between subjects and hemispheres, continued study of HG morphology may lead to the identification of unique patterns. From this subject pool, patterns emerged in the differing configurations of SI, HS1, and MD. If this detailed protocol for labeling HG is employed in investigations with larger sample sizes, the variability in HG might become more predictable, and more distinct patterns in its gyrification may solidify. Furthermore, unedited and edited labels can be compared in the future to examine the impact--and thus, necessity--of manual editing on final HG volumes. It is important to note that, while examining and labeling the boundaries of each HG individually lead to a higher degree of accuracy, the process is time consuming and inefficient. It is unlikely that a tedious labeling system would be widely adopted for

diagnostic purposes by researchers and clinicians. However, results from the use of this protocol in a larger sample of brains could lead to the development of an atlas or more nuanced probabilistic-mapping algorithms for labeling the superior temporal plane. This would allow for more efficient and accessible labeling methods and hopefully increase the accuracy and consistency in future morphological studies.

4.3 Limitations and Future Directions

An important consideration in generalizing these results is the relatively small sample size of this study. Dyslexia may have heterogeneous origins, with a potential origin being related to multiple convolutions (≥ 3) of HG in the right and/or left hemispheres. All morphotypes, aside from MD, occurred at similar proportions in both hemispheres of both groups. It is possible that the similarity in HG duplication between these brains occurred by coincidence and that a more diverse sample would elevate differences between the groups. Given the overall rarity of the MD morphotype, a larger sample size might help to demonstrate a significant preference for MD duplications in the dyslexic brain. The results of this study were hindered by a small number of MD in control brains which may have influenced the significant effect of morphotype in dyslexic brains. Larger group numbers would increase statistical power and possibly show more significant differing patterns of HG duplication between control and dyslexic brains.

Along with a larger sample size, future studies should include additional labeling and morphometric analyses. Overall, the type of HG duplication was not significantly different between control and dyslexic brains. Measurements of surface area and curvature would allow us to identify if other morphological differences exist between dyslexic and

control brains. Additionally, total HG volume was not significantly lateralized to either hemisphere. However, it is known that language is left-lateralized in the general population (Tzourio-Mazoyer & Mazoyer, 2017). In left-lateralized individuals, PT is large in the left hemisphere and sometimes nonexistent in the right. It would be interesting to confirm if HG reduplication leads to a decrease in PT volume or surface area, based solely on macrostructural landmarks. Altarelli et al. (2014) have previously investigated PT in dyslexic children and found altered patterns of asymmetry in dyslexic boys. It would be interesting to replicate these findings and investigate if this pattern is maintained into adulthood. Future studies can establish an anatomical labeling protocol for PT and examine any morphometric differences that exist between control and dyslexic brains, or that are influenced by reduplication of HG.

Considering the amount of variability between individual brains, anatomical landmarks might be more clearly defined by their functional connections than their structure (Saygin et al., 2012). Diffusion tensor imaging (DTI), specifically diffusion-weighted imaging, can be used to map white matter tractography and identify how activated regions are connected during reading tasks (Ramus et al., 2018). Understanding connectivity, along with regional activation, during functional brain imaging studies could give more insight into the areas that are impaired or disrupted in the dyslexic brain.

Finally, the gold standard in behavioral investigations of dyslexia is to conduct longitudinal studies which follow at-risk children into adulthood (Ramus et al., 2018). Longitudinal studies allow investigators to distinguish between pre-existing neural abnormalities and any adaptations or disruptions that occur in the brain after reading skills

are acquired. This is important to consider because reading is a behavior driven by culture versus survival (Perrachione et al., 2016). It follows that the circuitry for reading is not an innate adaptation that is present in the pediatric brain and that years of reading behavior might lead to significant changes in the networks and regions that support reading prerequisites, such as rapid neural adaptation, visual attention, and phonological processing. The brains of children identified as at-risk for reading disorders may show baseline abnormalities that are disguised by years of reading training in the adult brain (Kraft et al., 2016). Further, not all at-risk children go on to develop a reading disorder. Only by following these children well into their years of reading instruction can dyslexia be confirmed. Longitudinal studies can also provide additional insight into neural plasticity and if and how the dyslexic brain compensates.

CONCLUSION

When labeling anatomical structures in the brain, it is important to develop and adopt specific, detailed protocols in order to reach a consensus within the research community. Our protocol for labeling HG sought to be less biased by following prominent gyri and sulci instead of assigning labels according to hypothesized resident cortices (e.g., primary auditory cortex, auditory association cortices). Because brain morphology is highly variable between individuals, our labeling scheme was specific but flexible and included four different morphotypes: single gyrus, common-stem duplication, complete posterior duplication, and multiple duplications.

The results of this study have shown that reduplication of HG alone is not enough to distinguish between control and dyslexic brains. Duplicated patterns of HG occur frequently in the general population and are not, in themselves, indicative of abnormal brain development or behavioral impairments. Morphometric measurements, such as gray matter volume, surface area and curvature, and white matter tractography, could provide a more nuanced picture of structure and functional connectivity. It is likely that developmental dyslexia is the cumulative product of innate altered patterns of connectivity throughout the language systems of the brain. In remediated adults with developmental dyslexia, reading skill is influenced by these comorbid differences along with compensations that the brain has developed after years of training. Understanding how the dyslexic brain fundamentally differs from controls, along with how it changes to adapt for reading behavior could provide an avenue for earlier, more accurate diagnosis and more targeted treatment. Future research might explore how the neural reading network changes

from child to adulthood and how duplications of HG, defined by the labeling protocol used in this study, affect the size of PT and its connections to regions important for reading fluency.

REFERENCES

Abdul-Kareem, I. A. & Sluming, V. (2008). Heschl gyrus and its included auditory cortex: Structural MRI studies in healthy and diseased subjects. *Journal of Magnetic Resonance Imaging, 28,* 1–29.

Altarelli, I., Leroy, F., Monzalvo, K., Fluss, J., Billard, C., Dehaene-Lambertz, G. … Ramus, F. (2014). Planum temporale asymmetry in developmental dyslexia: Revisiting an old question. *Human Brain Mapping, 35*, 5717–5735.

Benner, J., Wengenroth, M., Reinhardt, J., Stippich, C., Schneider, P., & Blatow, M. (2017). Prevalence and function of Heschl's gyrus morphotypes in musicians. *Brain Structure and Function, 222,* 3587–3603.

Da Costa, S., van der Zwaag, W., Marques, J. P., Frackowiak, R. S. J., Clarke, S., & Saenz, M. (2011). Human primary auditory cortex follows the shape of Hesch's gyrus. *The Journal of Neuroscience, 31,* 14067–14075.

Dale, A. M., Fischl, B., & Sereno, M. I. (1999). Cortical surface-based analysis. I. Segmentation and surface reconstruction. *Neuroimage, 9,* 179–194.

DuBois, J., Benders, M., Borradori-Tolsa, C., Lazeyras, F., Leuchter, R. H-V., Sizonenko, S. V. … Hüppi, P. S. (2008). Primary cortical folding in the human newborn: An early marker for later functional development. *Brain, 131,* 2028–2041.

Eckhert, M. A., Berninger, V. W., Vaden, K. I., Gebregziabher, M., & Tsu, L. (2016). Gray matter features of reading disability: A combined meta-analytic and direct analysis approach. *eNeuro, 3,* 1–15.

Gaser, C., Nenadic, I., Volz, H-P., Büchel, C., & Sauer, H. (2004). Neuroanatomy of 'hearing voices': A frontotemporal brain structural abnormality associated with auditory hallucinations in schizophrenia. *Cerebral Cortex, 14,* 91–96.

Ghosh, S. S., Kakunoori, S., Augustinack, J., Neito-Castanon, A., Kovelman, I., Gaab, N. … Fischl, B. (2010). Evaluating the validity of volume-based and surface-based image registration for developmental cognitive neuroscience studies in children 4 to 11 years of age. *NeuroImage, 53,* 85–93.

Golestani, N. & Pallier, C. (2007). Anatomical correlates of foreign speech sound production. *Cerebral Cortex, 17,* 929–934.

Golestani, N., Molko, N., Dehaene, S., LeBihan, D., & Pallier, C. (2007). Brain structure predicts the learning of speech sounds. *Cerebral Cortex, 17,* 17575–17582.

Golestani, N., Price, C. J., & Scott, S. K. (2011). Born with an ear for dialects? Structural plasticity in the expert phonetician brain. *Journal of Neuroscience, 3,* 4213–4220.

Hirayasu, Y., McCarley, R. W., Salisbury, D. F., Tanaka, S., Kwon, J. S., Frumin, M. … Shenton, M. E. (2000). Planum temporale and Heschl gyrus volume reduction in schizophrenia. *Archives of General Psychiatry, 57,* 692–699.

Kraft, I., Schreiber, J., Cafiero, R., Metere, R., Schaadt, G., Brauer, J. … Skeide, M. A. (2016). Predicting early signs of dyslexia at preliterate age by combining behavioral assessment with structural MRI. *NeuroImage, 143,* 378–386.

Leonard, C., Eckert, M., Given, B., Virginia, B., & Eden, G. (2006). Individual differences in anatomy predict reading and oral language impairments in children. *Brain, 129,* 3329–3342.

Leonard, C. M., Eckert, M. A., Lonbardino, L. J., Oakland, T., Kranzler, J., Mohr, C. M. … Freeman, A. (2001). Anatomical risk factors for phonological dyslexia. *Cerebral Cortex, 11*, 148–157.

Leonard, C. M., Puranik, C., Kuldau, J. M., & Lombardino, L. J. (1998). Normal variation in the frequency and location of human auditory cortex landmarks. Heschl's gyrus: Where is it? *Cerebral Cortex, 8,* 397–406.

Leonard, C., Voeller, K. S., Lombardino, L., Morris, M. K., Alexander, A., Anderson, H. … Staab, E. (1993). Anomalous cerebral structure in dyslexia revealed with magnetic resonance imaging. *Archives of Neurology, 50,* 461–469.

Lervåg, A. & Hulme, C. (2009). Rapid automatized naming (RN) taps a mechanism that places constraints on the development of early reading fluency. *Psychological Science, 20,* 1040–1048.

Marie, D., Jobard, G., Crivello, F., Perchey, G., Petit, L., Mellet, E. … Tzourio-Mazoyer, N. (2015). Descriptive anatomy of Heschl's gyri in 430 healthy volunteers, including 198 left-handers. *Brain Structure and Function, 220*, 729–743.

Norton, E. S., Beach, S. D., & Gabrieli, J. D. E. (2015). Neurobiology of dyslexia. *Current Opinion in Neurobiology, 30,* 73–78.

Penhune, V. B., Zatorre, R. J., MacDonald, J. D., & Evans, A. C. (1996). Interhemispheric anatomical differences in human primary auditory cortex: Probabilistic mapping and volume measurement from magnetic resonance scans. *Cerebral Cortex, 6,* 661–672.

Perrachione, T. K., Del Tufo, S. N., Winter, R., Murtagh, J., Cyr, A., Chang, P … Gabrieli, J. D. E. (2016). Dysfunction of rapid neural adaptation in dyslexia. *Neuron, 92,* 1383–1397.

Rademacher, J., Caviness, V. S., Steinmetz, H., & Galaburda A. M. (1993). Topographical variation of the human primary auditory cortices: Implications for neuroimaging, brain mapping, and neurobiology. *Cerebral Cortex, 3,* 313–329.

Ramus, F., Altarelli, I., Jednoróg, K., Zhao, J., & Scotto di Covella, L. (2018). Neuroanatomy of developmental dyslexia: Pitfalls and promise. *Neuroscience and Biobehavioral Reviews, 84,* 434–452.

Saygin, Z. M., Osher, D. E., Koldewyn, K., Reynolds, G., Gabrieli, J. D. E., & Saxe, R. R. (2011). Anatomical connectivity patterns predict face selectivity in the fusiform gyrus. *Nature Neuroscience, 15*, 321–327.

Schneider, P., Scherg, M., Dosch, H. G., Specht, H. J., Gutschalk, A., & Rupp, A. (2002). Morphology of Heschl's gyrus reflects enhanced activation in the auditory cortex of musicians. *Nature Neuroscience, 5,* 688–694.

Schneider, P., Sluming, V., Roberts, N., Scherg, M., Goebel, R., Specht, H. J. … Rupp, A. (2005). Structural and functional asymmetry of later Heschl's gyrus reflects pitch perception preference. *Nature Neuroscience, 8,* 1241–1247.

Shapleske, J., Rossell, S. L., Woodruff, P. W. R., & David, A. S. (1998). The planum temporale: A systematic, quantitative review of its structural, functional, and clinical significance. *Brain Research Reviews, 29,* 26–49.

Shaywitz, S. E. (1989). Dyslexia. *New England Journal of Medicine, 338,* 307–312.

Shaywitz, S. E. & Shaywitz, B. A. (2003). Dyslexia (Specific reading disability). *Pediatrics in Review, 24,* 147–153.

Smiley, J. F., Hackett, T. A., Preuss, T. M., Bleiwas, C., Figarsky, K., Mann, J. J. … Dwork, A. J. (2013). Hemispheric asymmetry of primary auditory cortex and Heschl's gyrus in schizophrenia and nonpsychiatric brains. *Psychiatric Research: NeuroImaging, 214,* 435–443.

Smiley, J. F., Rosoklija, G., Mancevski, B., Mann, J. J., Dwork, A. J., & Javitt, D. C. (2009). Altered volume and hemispheric asymmetry of the superficial cortical layers in the schizophrenia planum temporale. *European Journal of Neuroscience, 30,* 449–463.

Sumich, A., Chitnis, X. A., Fannon, D. G., O'Ceallaigh, S., Doku, V. C., Faldrowicz, A., & Sharma, T. (2005). Unreality symptoms and volumetric measures of Heschl's

gyrus and planum temporale in first-episode psychosis. *Biological Psychiatry, 57,* 947–950.

Torgesen, J. K., Wagner, R. K., & Rashotte, C. A. (1999). *Test of Word Reading Efficiency* (TOWRE). Austin, TX: Pro–Ed. (1999).

Tzourio-Mazoyer, N. & Mazoyer, B. (2017). Variations of planum temporale asymmetries with Heschl's gyri duplications and association with cognitive abilities: MRI investigations of 428 volunteers. *Brain Structure and Function, 22,* 2711–2726.

Waldie, K. E., Wilson, A. J., Roberts, R. P., & Moreau, D. (2017). Reading network in dyslexia: Similar, yet different. *Brain & Language, 174,* 29–41.

Warrier, C., Wong, P., Penhune, V., Zatorre, R., Parrish, T., Abrams, D. … Kraus, N. (2009). Relating structure to function: Heschl's gyrus and acoustic processing. *The Journal of Neuroscience, 29,* 61–69.

Wengenroth, M., Blatow, M., Heinecke, A., Reinhardt, J., Stippich, C., Hofmann, E., & Schneider, P. (2014). Increased volume and function of right auditory cortex as a marker for absolute pitch. *Cerebral Cortex, 24,* 1127–1137.

Wong, P. C. M., Warrier, C. M., Penhune, V. B., Roy, A. K., Sadehh, A., Parrish, T. B., & Zatorre, R. J. (2008). Volume of left Heschl's gyrus and linguistic pitch learning. *Cerebral Cortex, 18*, 828–836.

Woodcock, R. W. (1998). *Woodcock Reading Mastery Tests – Revised/Normative Update* (WRMT-R/NU). Circle Pines, MN: American Guidance Service.

Yamasaki, S., Yamasue, H., Abe, O., Yamada, H., Iwanami, A., Hirayasu, Y. … Kasai, K. (2007). Reduced planum temporale volume and delusional behaviour in patients with schizophrenia. *European Archives of Psychiatry and Clinical Neuroscience, 257,* 318–324.

Yousry, T.A., Fesl, G., Büttner, A., Noachtar, S., & Schmid, U.D. (1997). Heschl's gyrus: Anatomic description and methods of identification on magnetic resonance imaging. *International Journal of Neuroradiology, 3*, 2–12.

Zatorre, R. J. (2003). Absolute pitch: A model for understanding the influence of genes and development on neural and cognitive function. *Nature Neuroscience, 6,* 692–695.

VITA